Title

Hsf1 promotes hematopoietic stem cell fitness and proteostasis in response to ex vivo culture stress and aging

Journal

Cell Stem Cell, 28(11)

ISSN

1934-5909

Authors

Kruta, Miriama
Sunshine, Mary Jean
Chua, Bernadette A
et al.

Publication Date

2021-11-01

DOI

10.1016/j.stem.2021.07.009

Peer reviewed

HHS Public Access

Author manuscript

Cell Stem Cell. Author manuscript; available in PMC 2022 November 04.

Published in final edited form as:

Cell Stem Cell. 2021 November 04; 28(11): 1950–1965.e6. doi:10.1016/j.stem.2021.07.009.

Hsf1 promotes hematopoietic stem cell fitness and proteostasis in response to ex vivo culture stress and aging

Miriama Kruta[1], **Mary Jean Sunshine**[1], **Bernadette A. Chua**[1], **Yunpeng Fu**[1], **Ashu Chawla**[2], **Christopher H. Dillingham**[1,2], **Lorena Hidalgo San Jose**[1], **Bijou De Jong**[1], **Fanny J. Zhou**[1], **Robert A.J. Signer**[1,3,*]

[1]Division of Regenerative Medicine, Department of Medicine, Moores Cancer Center, University of California San Diego, La Jolla, CA, 92093 USA.

[2]La Jolla Institute for Immunology, La Jolla, CA, 92037 USA.

[3]Lead contact

Summary

Maintaining proteostasis is key to resisting stress and to promoting healthy aging. Proteostasis is necessary to preserve stem cell function, but little is known about the mechanisms that regulate proteostasis during stress in stem cells, and whether disruptions in proteostasis contribute to stem cell aging is largely unexplored. We determined that ex vivo cultured mouse and human hematopoietic stem cells (HSCs) rapidly increase protein synthesis. This challenge to HSC proteostasis was associated with nuclear accumulation of Hsf1, and deletion of *Hsf1* impaired HSC maintenance ex vivo. Strikingly, supplementing cultures with small molecules that enhance Hsf1 activation partially suppressed protein synthesis, rebalanced proteostasis, and supported retention of HSC serial reconstituting activity. Although *Hsf1* was dispensable for young adult HSCs in vivo, *Hsf1* deficiency increased protein synthesis and impaired the reconstituting activity of middle-aged HSCs. Hsf1 thus promotes proteostasis and the regenerative activity of HSCs in response to culture stress and aging.

Graphical Abstract

*Correspondence: Robert A.J. Signer, UC San Diego Moores Cancer Center, 3855 Health Sciences Drive, La Jolla, CA 92093-0652, USA, Tel: 858-534-0732, rsigner@ucsd.edu, Twitter: @SignerLab.

Author Contribution

R.A.J.S. conceived the project and wrote the manuscript. M.K. and R.A.J.S. designed, performed, and analyzed experiments. M.S. supported mouse breeding, tissue processing, cell culture and transplantation. B.A.C. and L.H.S. performed/analyzed proteostasis experiments. A.C. and F.Z. performed computational analysis. Y.F., C.H.D. and B.D.J provided technical support.

Author Information

A patent resulting from this work has been filed. The authors declare no other competing financial interests.

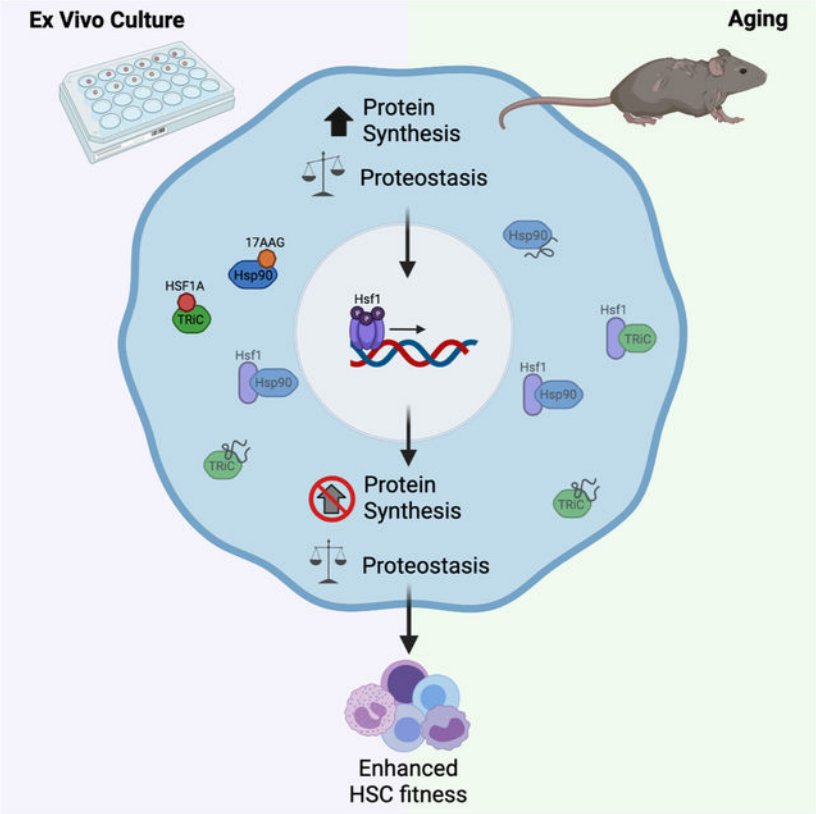

eTOC Blurb

Inability to grow HSCs in culture is a major barrier to their expanded use in cell-based therapies. Kruta et al. demonstrate that cultured HSCs rapidly increase protein synthesis, which severely disrupts proteostasis and impairs their self-renewal. Hsf1 activation promotes HSC fitness and proteostasis in culture and during aging in vivo.

Keywords

stem cell; hematopoietic stem cell; stress; proteostasis; Hsf1; heat shock response; protein synthesis; translation; aging; hematopoiesis

Introduction

Hematopoietic stem cells (HSCs) regenerate blood and immune cells throughout life. To maintain life-long stem cell function and tissue integrity, HSCs depend on specialized stress response mechanisms to mitigate replicative (Alvarez et al., 2015; Flach et al., 2014; Xiao et al., 2012), metabolic (Gan et al., 2010; Gurumurthy et al., 2010; Karigane et al., 2016; Mohrin et al., 2015; Nakada et al., 2010; Takubo et al., 2013; Yu et al., 2013), oxidative (Abbas et al., 2010; Ito et al., 2004; Ito et al., 2006; Maryanovich et al., 2015; Tothova et al., 2007) and genotoxic stress (Beerman et al., 2014; Milyavsky et al., 2010; Mohrin et al., 2010; Rossi et al., 2007; Walter et al., 2015; Wang et al., 2012). HSCs may also be subject to significant protein stress (Chambers et al., 2007; Chua et al., 2020), and the ability to

respond to these acute and chronic stressors is critical to maintaining protein homeostasis (proteostasis). However, little is yet known about the factors that regulate proteostasis during stress in stem cells (Chua and Signer, 2020).

A primary response to protein stress in the cytoplasm is activation of the heat shock response (Akerfelt et al., 2010). The master regulator of this pathway is *Heat shock factor 1* (*Hsf1*), which encodes a highly conserved transcription factor that promotes proteostasis maintenance (Anckar and Sistonen, 2011). At steady state, inactive Hsf1 is localized in the cytoplasm where it binds to chaperones (Neef et al., 2014; Shi et al., 1998; Zou et al., 1998). Under conditions of protein stress, the chaperones dissociate from Hsf1 to bind unfolded/misfolded proteins. This enables Hsf1 to translocate to the nucleus where it classically induces transcription of heat shock proteins – molecular chaperones that coordinate protein folding, trafficking and degradation to enhance proteostasis and promote cell survival (Anckar and Sistonen, 2011; Mendillo et al., 2012).

We previously discovered that young adult HSCs have lower protein synthesis rates than other hematopoietic cells (Signer et al., 2014). Low protein synthesis is necessary for adult HSC maintenance, as modest increases in protein synthesis disrupt proteostasis and impair self-renewal in vivo (Hidalgo San Jose et al., 2020; Magee and Signer, 2021; Signer et al., 2014; Signer et al., 2016). Here, we report that ex vivo culture rapidly induces a massive increase in protein synthesis within mouse and human HSCs that disrupts proteostasis. This protein stress induces accumulation of Hsf1 in the nucleus of cultured HSCs, and deletion of *Hsf1* severely impairs their long-term multilineage reconstituting activity. Supplementing cultures with small molecules that enhance Hsf1 activation partially suppresses protein synthesis, rebalances proteostasis, and supports sustained ex vivo HSC maintenance. Finally, we found that Hsf1 is activated within middle-aged HSCs in vivo where it suppresses protein synthesis and promotes long-term multilineage reconstituting activity.

Protein synthesis is elevated within ex vivo cultured HSCs

To initiate our studies, we sought to identify a model to study the regulation of proteostasis within HSCs in response to stress. We began by examining the effects of cell culture stress on HSCs. To gain an unbiased view of the cell intrinsic changes that occur within HSCs in culture, we performed RNA-sequencing on $CD150^{+}CD48^{-}Lineage^{-}Sca1^{+}ckit^{+}$ ($CD150^{+}CD48^{-}LSK$) HSCs (Kiel et al., 2005) (Fig. S1A,B) that were freshly isolated from young adult (2-3-month-old) mice as well as HSCs that were cultured ex vivo for 18 hours (h) in medium supplemented with Stem Cell Factor (SCF), Thrombopoietin (TPO), 2-Mercaptoethanol and bovine serum albumin (“basic HSC medium”; Fig. 1A). The 18h time point typically precedes the first HSC division in culture (Flach et al., 2014).

The transcripts of 2368 genes were changed by at least 2-fold (Padj<0.05) between freshly isolated and 18h-cultured HSCs (Fig. 1B, S1C,D). To sort through these transcriptional changes, we performed gene set enrichment analysis (Subramanian et al., 2005) for gene ontology terms describing biological processes (Table S1). The “Regulation of Cellular Response to Stress” gene set was significantly upregulated in cultured HSCs (Fig. 1C), indicating that ex vivo culture induces significant stress on HSCs.

Strikingly, several of the most upregulated gene sets in cultured HSCs were related to protein synthesis, including “Ribosome Biogenesis”, “mRNA Processing”, “Amino Acid Metabolic Process”, “Translation Initiation”, “Translation Elongation” and “Translation Termination” (Fig. 1D–I). These data raised the possibility that the regulation of protein synthesis was particularly disrupted within ex vivo cultured HSCs.

To directly test the effects of ex vivo culture on protein synthesis, we cultured HSCs for 4 or 18h and quantified protein synthesis based on O-propargyl-puromycin (OP-Puro) incorporation (Hidalgo San Jose and Signer, 2019; Liu et al., 2012; Signer et al., 2014). After 4h in culture, HSCs exhibited a 6.7-fold increase in protein synthesis as compared to HSCs in vivo (Fig. 1J). After 18h in culture, HSCs synthesized 19.4-fold more protein per hour than HSCs in vivo (Fig. 1J). Similarly, human cord blood $CD34^+$ hematopoietic stem and progenitor cells (HSPCs) cultured for 18h exhibited a 5.2-fold increase in protein synthesis compared to uncultured controls (Fig. 1K). These data indicate that mouse and human HSCs rapidly and significantly increase protein synthesis in culture.

Although HSCs in young adult bone marrow are predominantly quiescent (Cheshier et al., 1999), elevated protein synthesis within HSCs in culture could not be fully explained by increased cell cycle entry. HSCs in vivo can be driven to undergo rapid self-renewing divisions by treating mice with cyclophosphamide and granulocyte colony-stimulating factor (GCSF) (Morrison et al., 1997). Cycling HSCs in vivo exhibit a ~2-fold increase in protein synthesis compared to steady state quiescent HSCs (Fig. 1J) (Signer et al., 2014). HSCs cultured ex vivo for 18h thus produce ~10-fold more protein per hour than dividing HSCs in vivo (Fig. 1J).

Next, we tested whether large increases in protein synthesis in culture were unique to HSCs or could be broadly observed amongst hematopoietic progenitors. We cultured common myeloid progenitors (CMPs), granulocyte-macrophage progenitors (GMPs), and megakaryocyte-erythroid progenitors (MEPs) (Akashi et al., 2000) for 18h. CMPs and GMPs exhibited a ~2-fold increase in protein synthesis in culture as compared to in vivo (Fig. 1L). MEPs did not exhibit any significant change in protein synthesis after 18h in culture (Fig. 1L). HSCs which typically synthesize ~5-8-fold less protein per hour than CMPs, GMPs and MEPs in vivo (Signer et al., 2014), exhibited significantly higher protein synthesis than all these progenitor populations after 18h in culture (Fig. 1L). These data indicate that HSCs exhibit a particularly large increase in protein synthesis in culture.

The increase in protein synthesis within ex vivo cultured HSCs is particularly notable because HSCs in vivo require a highly-regulated protein synthesis rate (Magee and Signer, 2021; Signer et al., 2014). Adult HSCs exhibit lower protein synthesis than other hematopoietic cells in vivo, and modest increases (~30%) in protein synthesis can significantly disrupt proteostasis within HSCs and impair their function (Hidalgo San Jose et al., 2020; Signer et al., 2014; Signer et al., 2016).

Proteostasis is maintained partly through balanced protein synthesis and degradation. Despite a 19.4-fold increase in protein synthesis, cultured HSCs exhibited no significant change in proteasome activity as compared to freshly isolated HSCs (Fig. 1M). Given

this discrepancy between protein synthesis and degradation activity, we used Ub^{G76V}-*GFP* reporter mice (Lindsten et al., 2003) to test if proteostasis becomes unbalanced within cultured HSCs (Fig. 1N). Ub^{G76V}-*GFP* mice ubiquitously express GFP that is fused to a constitutively active degradation signal. *GFP* transcripts can be detected, but no fluorescence is detected because GFP is rapidly degraded by the proteasome. We previously established that increased protein synthesis and/or accumulation of misfolded/unfolded proteins could overwhelm proteasome capacity and unbalance proteostasis within HSCs in vivo, which is marked by accumulation of GFP (Hidalgo San Jose et al., 2020). Ub^{G76V}-*GFP* HSCs cultured for 18h exhibited more than 10-fold accumulation of GFP as compared to HSCs in vivo (Fig. 1O). Thus, ex vivo culture severely increases protein synthesis and unbalances proteostasis within HSCs at a magnitude that cannot be tolerated in vivo.

Hsf1 promotes ex vivo HSC maintenance

Ex vivo cultured HSCs exhibited significant upregulation of the “Response to Heat” gene set as compared to fresh HSCs (Fig. 2A), suggesting that they may activate the heat shock response. The heat shock response is a central cellular response to protein stress in the cytoplasm (Akerfelt et al., 2010), and is controlled by the transcription factor *Hsf1* (Anckar and Sistonen, 2011). At steady state, inactive Hsf1 is sequestered in the cytoplasm through interactions with chaperones, including Hsp90 and TRiC (Neef et al., 2014; Shi et al., 1998; Zou et al., 1998) (Fig. 2B), which are highly expressed by HSCs (Fig. 2D). Under conditions of protein stress, the chaperones bind unfolded/misfolded proteins (Fig. 2C), enabling Hsf1 to translocate to the nucleus where it promotes a transcriptional response aimed at restoring proteostasis and promoting cell survival (Anckar and Sistonen, 2011; Mendillo et al., 2012) (Fig. 2C).

Hsf1 is highly expressed by young adult HSCs in vivo (Fig. 2D), but the protein is largely absent from the nucleus (Fig. 2E), suggesting that it is likely inactive as a transcription factor at steady state. In contrast, we observed a significant accumulation of Hsf1 within the nucleus of ex vivo cultured young adult mouse HSCs (Fig. 2E,F) and human cord blood $CD34^+$ HSPCs (Fig. 2G,H). The accumulation of Hsf1 in the nucleus of cultured HSCs could not be explained by increased gene expression, as the abundance of *Hsf1* mRNA was similar between fresh and cultured HSCs (Fig. 2I). These data suggest that protein stress in culture led to nuclear Hsf1 accumulation in HSCs.

We thus tested whether Hsf1 influences ex vivo HSC maintenance. To do this, we conditionally deleted *Hsf1* from hematopoietic cells by treating 6-week-old $Hsf1^{fl/fl}$;*Mx1-Cre*$^+$ (*Hsf1*-deficient) or control $Hsf1^{fl/fl}$ mice with polyinosine:polycytidine (pIpC). We confirmed that *Hsf1* was deleted from >95% of HSCs (not shown). Seven days after pIpC administration, when HSCs returned to steady state (Essers et al., 2009), $CD150^+CD48^-$LSK HSCs were sorted from the bone marrow of *Hsf1*-deficient and control mice into 96-well plates at a density of 10 cells/well, and cultured in basic HSC medium for 10 days (d) without any medium change or passaging (Fig. 2J). After 10d in culture, both *Hsf1*-deficient and control HSCs expanded into ~25,000 cells (Fig. 2K), and we competitively transplanted the complete cellular contents of each well together with 2×10^5 fresh wild-type congenic bone marrow cells into irradiated mice. Overall, cultured *Hsf1*-

deficient HSCs exhibited a severe loss of reconstituting activity as compared to controls (Fig. 2L–P). Only 8/30 (27%) recipients of cultured *Hsf1*-deficient HSCs exhibited long-term multilineage reconstitution as compared to 23/36 (64%) recipients of cultured control HSCs (Fig. 2Q).

Defects in cultured *Hsf1*-deficient HSCs do not reflect a requirement for *Hsf1* within young adult HSCs in vivo. 2-month-old *Hsf1*-deficient mice had normal bone marrow cellularity (Fig. S2A), and the frequencies of HSCs and progenitors were unchanged compared to controls (Fig. S2B–F). To test whether Hsf1 is necessary to regulate HSC function in young adult mice, we competitively transplanted 10 freshly isolated *Hsf1*-deficient or control HSCs with 2×10^5 congenic bone marrow cells into irradiated mice. After 16 weeks, 3×10^6 bone marrow cells from primary recipients were serially transplanted into irradiated mice (Fig. S2G). Overall, long-term hematopoietic reconstitution from *Hsf1*-deficient HSCs that were freshly isolated from 2-month-old mice was statistically indistinguishable from controls in both primary and secondary recipients (Fig. S2H–J). *Hsf1*-deficiency also did not significantly affect HSPC homing to the bone marrow (Fig. S2K). Consistent with a previous report (Kourtis et al., 2018), these data indicate that *Hsf1*-deficiency does not influence the maintenance, reconstituting activity or self-renewal of young adult HSCs in vivo. Hsf1 thus promotes the maintenance of young adult HSCs ex vivo but not in vivo.

17-AAG and HSF1A enhance the serial reconstituting activity of ex vivo cultured HSCs

Since Hsf1 promotes ex vivo HSC maintenance, we wondered if further increasing Hsf1 activity could improve ex vivo HSC growth. Small molecule inhibitors of Hsp90 or TRiC can prevent their association with Hsf1 and induce Hsf1 nuclear translocation (Fig. 3A) (Neef et al., 2014; Neef et al., 2010; Schulte and Neckers, 1998). We determined that this activity is operative within mouse and human HSCs, as culturing HSCs in the presence of the Hsp90 inhibitor Tanespimycin (17-N-allylamino-17-demethoxygeldanamycin, 17-AAG) or the TRiC inhibitor HSF1 Activator (HSF1A) significantly enhanced nuclear accumulation of Hsf1 after 18h or 10d of culture (Fig. 3B–F, S3A–C).

Next, we tested if 17-AAG or HSF1A could enhance the reconstituting activity of cultured HSCs. HSCs were sorted from 2-3-month-old mice into 96-well plates (10/well) containing basic HSC medium supplemented with either 17-AAG, HSF1A or vehicle (DMSO) (Fig. 3G). Over the 10d culture period, HSCs in all culture conditions proliferated extensively, and expanded into ~$1.5–2\times10^4$ cells (Fig. S4A). After 10d, the cellular contents of each well were competitively transplanted with 2×10^5 fresh congenic bone marrow cells into irradiated mice.

17-AAG and HSF1A consistently enhanced the long-term multilineage reconstituting activity of cultured HSCs, although the differences did not always reach the threshold of statistical significance (Fig. 3H–L, S3D–H). Recipients of HSCs cultured with 17-AAG and HSF1A also exhibited a trend toward increased engraftment of donor-derived hematopoietic cells and HSCs in the bone marrow 16 weeks after transplant (Fig. S3O–S).

Since retention of serial long-term multilineage reconstituting potential is the critical barrier for ex vivo HSC culturing protocols (Purton and Scadden, 2007), we performed secondary transplants. Strikingly, HSCs cultured with either 17-AAG or HSF1A gave significantly more reconstitution in the peripheral blood and bone marrow of secondary recipients than controls (Fig. 3M–R, S3I–N, S3T–W). Overall, 31/37 (85%) and 22/33 (67%) secondary recipients of HSCs cultured with 17-AAG and HSF1A, respectively, exhibited long-term multilineage reconstitution as compared to just 11/32 (34%) recipients of HSCs cultured with DMSO (Fig. 3R, S3N). These data demonstrate that 17-AAG and HSF1A significantly enhance the serial long-term multilineage reconstituting activity of ex vivo cultured HSCs.

HSCs cultured with 17-AAG and HSF1A are functionally similar to fresh HSCs

The increased serial reconstituting activity of HSCs cultured with 17-AAG and HSF1A raised the question of whether this reflected HSC expansion or improved maintenance. To test this, we quantified $CD150^{+}CD48^{-}$LSK cells present after 10d of culture. The number of $CD150^{+}CD48^{-}$LSK cells was increased from 10 (day 0) to ~400–800 at day 10, but there was no significant difference between 17-AAG, HSF1A or control cultures (Fig. S4B). The frequencies of $CD48^{+}$LSK multipotent progenitors, $Lineage^{-}ckit^{+}Sca1^{-}$ myeloid progenitors, $Lineage^{-}$ progenitors and $Lineage^{+}$ cells in 10d cultures were also similar amongst all conditions (Fig. S4C–F). Human $CD34^{+}$ cells also expanded similarly in all culture conditions from 2000 to ~25,000 over the 10d culture (Fig. S4G,H).

Since the $CD150^{+}CD48^{-}$LSK phenotype may not reliably mark HSCs ex vivo (Zhang and Lodish, 2005), we quantified functional HSCs in 17-AAG supplemented cultures by performing a limiting dilution assay (Hu and Smyth, 2009). Based on a previous report, cultures initiated with 10 $CD150^{+}CD48^{-}$LSK cells contain ~4.7 long-term repopulating units (Kiel et al., 2005). After 10d of culture, we detected an average of 6 repopulating units per well (Fig. S4I). These data indicate that 17-AAG on its own does not support significant HSC expansion, but rather supports HSC maintenance for at least 10d under conditions that are permissive for extensive proliferation and differentiation.

To further examine the effectiveness of 17-AAG and HSF1A on HSC fitness, we tested how well cultured HSCs function as compared to freshly isolated HSCs. To do this, additional cohorts of mice were transplanted with 10 freshly isolated HSCs together with 2×10^{5} congenic bone marrow cells (Fig. 4A). HSCs cultured with 17-AAG gave significantly higher levels of reconstitution than freshly isolated HSCs (Fig. 4B–F). HSCs cultured with HSF1A also gave modestly higher reconstitution than fresh HSCs, but the effect was less significant than with 17-AAG (Fig. S4J–N). Remarkably, HSCs cultured with either 17-AAG or HSF1A also gave similar levels of long-term multilineage reconstitution in secondary transplants as compared to fresh HSCs (Fig. 4G–K, S4O–S). These data indicate that 17-AAG and HSF1A support sustained ex vivo maintenance of HSCs capable of robust long-term multilineage reconstituting activity through multiple rounds of transplantation at levels equivalent to or greater than freshly isolated HSCs.

Effects of 17-AAG and HSF1A on ex vivo cultured HSCs largely require Hsf1

Although 17-AAG and HSF1A have distinct primary targets (Neef et al., 2010; Schulte and Neckers, 1998), they both increase nuclear expression of Hsf1 (Fig. 3B–F, S3B,C) and enhance the reconstituting activity of cultured HSCs (Fig. 3H–R, S3D–N). Together with our finding that Hsf1 promotes ex vivo HSC maintenance (Fig. 2L), these data strongly suggest that 17-AAG and HSF1A promote ex vivo HSC maintenance by enhancing Hsf1 activity. To directly test this, we examined the effects of 17-AAG and HSF1A on the reconstituting activity of cultured *Hsf1*-deficient HSCs.

HSCs were sorted from 2-month-old *Hsf1*-deficient and control mice (10/well) and cultured for 10d in basic HSC medium with either 17-AAG, HSF1A or DMSO. After 10d, the cellular contents of each well were competitively transplanted with 2×10^5 fresh congenic bone marrow cells into irradiated mice (Fig. 5A). *Hsf1*-deficient HSCs cultured in the presence of either 17-AAG or HSF1A gave much lower levels of hematopoietic reconstitution than control HSCs cultured under the same conditions (Fig. 5B, S5A). Furthermore, neither 17-AAG nor HSF1A had any effect on the reconstituting activity of *Hsf1*-deficient HSCs (Fig. 5C–F, S5B–E). These data demonstrate that the positive effect of 17-AAG and HSF1A on ex vivo HSC maintenance is dependent on the presence of Hsf1.

Since 17-AAG is an Hsp90 inhibitor that could have pleiotropic effects on HSCs, we sought to determine to what extent its transcriptional effects were mediated by Hsf1. We performed RNA-sequencing on wild-type and *Hsf1*-deficient HSCs cultured for 4h in basic HSC medium with 17-AAG or DMSO (Fig. 6A,B, S6A). RNA-sequencing at the 4h time point gave us the best opportunity to identify some of the earliest and primary transcriptional effects of 17-AAG on cultured HSCs.

Differential gene expression analysis revealed 17 protein coding genes whose expression was significantly increased (≥1.5-fold; Padj<0.05) within wild-type HSCs cultured with 17-AAG as compared to controls (Table S2). Eight (47%) out of those genes have previously been reported to be regulated by Hsf1 (Kovacs et al., 2019). In contrast to wild-type HSCs, 17-AAG only increased the expression of 4 protein coding genes within cultured *Hsf1*-deficient HSCs (Table S2), and only 1/4 (*Basp1*) was amongst the 17 genes whose expression was significantly increased by 17-AAG in wild-type cells. These data indicate that many of the early transcriptional effects of 17-AAG on cultured HSCs depend upon Hsf1.

Hsf1 and 17-AAG promote proteostasis maintenance within ex vivo cultured HSCs

To gain additional insight into the role of Hsf1 on ex vivo HSC maintenance, we sought to identify genes whose expression was upregulated in association with Hsf1 activation. Transcripts of 55 protein coding genes were significantly increased (≥1.5-fold; Padj<0.05) in cultured (4h) wild-type as compared to *Hsf1*-deficient HSCs (Fig. 6C, Table S3). 28 (51%) of these genes have previously been reported to be regulated by Hsf1 (Kovacs et al., 2019),

suggesting that Hsf1 has both established and previously undescribed transcriptional targets in HSCs.

Next, we determined that 7 of these prospective Hsf1 target genes exhibited further increased expression (≥1.1-fold) within wild-type cultured HSCs when 17-AAG was added to the culture (Fig. 6D). Four of these genes have previously been reported to be Hsf1 targets (Kovacs et al., 2019), and two - *Hspa1a* and *Tgm2* - are well established regulators of proteostasis that have not been characterized in HSCs. *Hspa1a* encodes a chaperone protein that is not typically expressed by young adult HSCs or bone marrow cells in vivo (Fig. S6B), and thus may have an unappreciated role in proteostasis regulation in HSCs under stress. *Tgm2* is preferentially expressed by young adult HSCs as compared to bone marrow cells (Fig. S6C), and has previously been reported to enhance Hsf1 activity by promoting its trimerization (Rossin et al., 2018). These data identify early transcriptional targets of Hsf1 whose expression is further increased by 17-AAG that could contribute to proteostasis maintenance within cultured HSCs.

To directly investigate the effects of Hsf1 and 17-AAG on HSC proteostasis, we assessed protein synthesis in wild-type and *Hsf1*-deficient HSCs cultured for 4h with 17-AAG or DMSO. *Hsf1*-deficient HSCs exhibited a modest, but significant increase in protein synthesis compared to controls (Fig. 6E). Furthermore, 17-AAG significantly reduced protein synthesis within cultured wild-type HSCs (Fig. 6E). However, 17-AAG also reduced protein synthesis within *Hsf1*-deficient HSCs, but protein synthesis was still significantly higher than in 17-AAG treated wild-type cells (Fig. 6E). Notably, 17-AAG and HSF1A continued to suppress protein synthesis within HSCs after 18h ex vivo, but had no effect on protein synthesis at this time point within *Hsf1*-deficient HSCs (Fig. S6D–G). These data indicate that Hsf1 suppresses protein synthesis within cultured HSCs, and that 17-AAG can further suppress protein synthesis partially through enhanced Hsf1 activation.

We also examined if Hsf1 and 17-AAG could promote rebalancing of proteostasis within cultured Ub^{G76V}-*GFP* HSCs. After 18h in culture, *Hsf1*-deficient Ub^{G76V}-*GFP* HSCs (Ub^{G76V}-GFP;$Hsf1^{fl/fl}$;*Mx1-Cre*$^{+}$) exhibited significantly more GFP positivity as compared to Ub^{G76V}-*GFP* controls (Fig. 6F). Furthermore, 17-AAG significantly reduced the frequency of GFP positive HSCs in culture (Fig. 6F). These data indicate that Hsf1 and 17-AAG promote the rebalancing of proteostasis within cultured HSCs.

Polyvinyl alcohol (PVA) was recently identified as a supplement that promotes ex vivo HSC expansion (Wilkinson et al., 2019). HSCs cultured for 18h with PVA exhibited reduced protein synthesis compared to BSA controls (Fig. S6H–J). Taken together with our 17-AAG and HSF1A experiments, these data suggest that interventions that promote ex vivo HSC growth are associated with a suppression of protein synthesis.

Hsf1-deficiency increases protein synthesis and impairs HSC function in vivo during aging

Next, we wondered whether Hsf1 could also regulate HSC function and proteostasis under conditions of protein stress in vivo. Loss of proteostasis is one of the hallmarks of aging

(Lopez-Otin et al., 2013), and is disrupted within some long-lived cell types such as neurons (Hipp et al., 2019; Kundra et al., 2017; Taylor and Dillin, 2011). Old adult HSCs express elevated levels of some heat shock proteins (Chambers et al., 2007), raising the possibility that aging HSCs experience protein stress in vivo. However, little is yet known about the factors that regulate proteostasis during HSC aging.

We assessed nuclear expression of Hsf1 within HSCs isolated from 3- and 22-month-old mice. In contrast to HSCs from 3-month-old mice, we observed substantial Hsf1 expression in the nucleus of HSCs from 22-month-old mice (Fig. 7A). Further, we determined that the accumulation of nuclear Hsf1 was already evident within HSCs isolated from 12-month-old mice (Fig. 7B). In agreement with these data, of the 55 genes that exhibited increased expression associated with Hsf1 activation ex vivo (Table S3), 38 (69%) tend to exhibit increased expression in old as compared to young adult HSCs (Young et al., 2021). These data indicate that Hsf1 is activated in middle-aged and old adult HSCs, and suggest that proteostasis is challenged within HSCs during aging.

Next, we tested whether Hsf1 influences hematopoiesis, protein synthesis and HSC function in middle-aged *Hsf1*$^{fl/fl}$;*Mx1-Cre*$^{+}$ mice. Similar to 3-month-old mice (Fig. S2B–F), 10-month-old *Hsf1*-deficient mice did not exhibit any significant changes in the frequency of HSCs or restricted progenitors as compared to age-matched controls (Fig. S7A–D). However, *Hsf1*-deficiency significantly increased protein synthesis within HSCs in 12-month-old mice (Fig. 7C, S7E). Hsf1 thus likely contributes to enabling aging HSCs to maintain low protein synthesis and proteostasis in vivo.

To test HSC function, we performed competitive bone marrow transplants. Consistent with our HSC transplants (Fig. S2H,I), recipients of 3-month-old *Hsf1*-deficient bone marrow cells had similar levels of reconstitution as controls in both primary and secondary transplants (Fig. 7D–M). However, primary recipients of 12-month-old *Hsf1*-deficient bone marrow cells showed a significant reduction in donor-derived cells in the blood over time as compared to age-matched controls (Fig. 7N–R). These data indicate that *Hsf1*-deficiency impairs HSC function during aging, and by middle age, Hsf1 is activated within HSCs where it contributes to attenuating protein synthesis and promoting their long-term multilineage reconstituting activity.

Discussion

It has historically been difficult to grow HSCs ex vivo (Kumar and Geiger, 2017). Even limited ex vivo growth typically leads to a loss of self-renewal activity and long-term multilineage differentiation potential (Bowman and Zon, 2009). This is a significant clinical problem because a sufficient source of HSCs is lacking for many patients that could benefit from HSC transplants (Copelan, 2006), and transplanting larger numbers of HSPCs increases the likelihood and speed of successful engraftment (Crane et al., 2017). In addition, the inability to grow HSCs ex vivo can limit the development and implementation of HSC gene correction therapies that are potentially curative for diverse genetic blood diseases (Naldini, 2015). Despite recent technical advances in HSC culturing protocols (Boitano et al., 2010; Calvanese et al., 2019; Eliasson et al., 2010; Fares et al., 2014;

Guo et al., 2018; Huang et al., 2012; Liu et al., 2015; Luchsinger et al., 2019; Mantel et al., 2015; Miharada et al., 2014; Wilkinson et al., 2019), we still have an incomplete understanding of why ex vivo growth impairs HSC self-renewal and engraftment. Our study indicates that ex vivo culture significantly increases protein synthesis within HSCs, and this disruption in proteostasis contributes to impaired HSC self-renewal and function. Activation of Hsf1 enables HSCs to better cope with culture induced protein stress and preserves their long-term multilineage reconstituting activity. 17-AAG and HSF1A mediated super-activation of Hsf1, and enhanced the maintenance of proteostasis and HSC fitness in culture. Similar to these findings with the heat shock response, activation of the unfolded protein response in either the endoplasmic reticulum or mitochondria can also promote HSC function in response to specific stressors (Mohrin et al., 2015; van Galen et al., 2018), but the role of these pathways in regulating ex vivo HSC growth has yet to be fully uncovered. Looking forward, identifying mechanisms and conditions that better support proteostasis maintenance could reveal new and improved approaches to grow, manipulate and expand HSCs ex vivo.

While Hsf1 is typically absent from the nucleus of young adult HSCs, it accumulates within the nucleus of HSCs during aging, suggesting that aging HSCs experience protein stress. The precise nature and origin of this stress remains largely unknown. Aged HSCs exhibit well-characterized features of aging, including accumulation of DNA damage (Beerman et al., 2014), telomere shortening (Allsopp et al., 2001), altered gene expression (Flach et al., 2014; Janzen et al., 2006; Sun et al., 2014), mitochondrial dysfunction (Mansell et al., 2021), increased reactive oxygen species (ROS) (Ito et al., 2006), and autophagy defects (Ho et al., 2017). Increased DNA damage in aged HSCs could lead to the production of altered transcripts that are translated into truncated or erroneous proteins susceptible to misfolding. ROS can oxidize proteins making them prone to unfolding (Ray et al., 2012). Aging HSCs exhibit increased transcription of ribosomal proteins and hypomethylation of rRNA, which could influence translation (Flach et al., 2014; Sun et al., 2014). Defects in autophagy can impair the degradation of misfolded proteins (Ciechanover and Kwon, 2015). Changes in the aging microenvironment, such as increased inflammation or altered growth factor production, may also influence HSC proteostasis (Pietras, 2017; Young et al., 2021). Moving forward, it is crucial to examine how these age-related changes influence HSC proteostasis, and to uncover additional mechanisms utilized by HSCs to cope with age-related protein stress. By doing so, there is a potential opportunity to reveal molecular strategies to manipulate proteostasis to enhance HSC fitness, improve tissue function and delay/prevent the onset of hematological diseases in older adults.

Limitations of the Study

Although heat shock can suppress protein synthesis (Lindquist, 1981), this typically occurs as a secondary effect that is independent of Hsf1 (Li et al., 2017). Our study revealed a more direct role for Hsf1 in suppressing protein synthesis within HSCs. However, the mechanism downstream of Hsf1 that contributes to suppressing translation remains to be uncovered.

In addition to its canonical role regulating the heat shock response, other context specific functions of Hsf1 have been reported, including metabolic reprogramming (Mendillo et al.,

2012) and changes to cytoskeletal integrity (Baird et al., 2014). In addition to proteostasis regulators, Hsf1 and 17-AAG induce gene expression changes that reflect non-canonical as well as undescribed functions of Hsf1. Intriguingly, one apparent target of Hsf1 within cultured HSCs is *Mllt3*, which has recently been shown to promote ex vivo HSC maintenance (Calvanese et al., 2019). Hsf1 may thus exert pleiotropic effects to promote maintenance of cultured HSCs that remain to be fully unraveled in future studies.

Similar to mouse HSCs, human cord blood HSPCs also experience significant protein stress in culture, marked by increased protein synthesis and nuclear accumulation of HSF1. 17-AAG and HSF1A enhance nuclear accumulation of HSF1 within human HSPCs, but whether they also enhance their engraftment remains to be determined. The effects of enhanced HSF1 activity as well as other interventions targeting the proteostasis network should be evaluated for their efficacy on human HSC function, but need to be combined with optimization of culture conditions. To maximize the likelihood of positively impacting human health, future studies on proteostasis in human HSCs should include systematic multiplexed analysis of medium composition, cytokine concentration, small molecule supplements, oxygen tension, culture duration and timing of cell passaging. Comprehensive optimization studies of this nature fall outside the scope of this study, but will be an exciting area of future investigation.

STAR METHODS

LEAD CONTACT

Further information and requests for resources and reagents should be directed to and will be fulfilled by the lead contact, Dr. Robert Signer (rsigner@ucsd.edu).

MATERIALS AVAILABILITY

This study did not generate new unique reagents.

DATA AND CODE AVAILABILITY

RNA-sequencing data have been deposited at GEO and are publicly available (GSE179415). Any additional information required to reanalyze the data reported in this paper is available from the lead contact upon request.

EXPERIMENTAL MODEL AND SUBJECT DETAILS

Mice—Mx1-*Cre* (Kuhn et al., 1995), *Hsf1*^{fl} (Le Masson et al., 2011) and Ub^{G76V}-*GFP* (Lindsten et al., 2003) mice have been described previously. Mice were all backcrossed for at least ten generations onto a C57BL background. C57BL6/J (CD45.2) and C57BL6.SJL (CD45.1) mice were used in transplantation experiments. Both male and female mice were used in all studies. Mice used in these studies were between 6 weeks and 22 months of age. For aging experiments, young adult mice were 2–3 months, middle-aged mice were 7–12 months and old mice were 22 months old. All mice were housed in the vivarium at the UC San Diego Moores Cancer Center. All protocols were approved by the UC San Diego Institutional Animal Care and Use Committee.

Cell isolation—Mouse bone marrow cells were isolated by flushing the long bones (femurs and tibias) or by crushing the long bones, vertebrae and pelvic bones with a mortar and pestle in Ca^{2+}- and Mg^{2+}- free Hank's buffered salt solution (HBSS; Corning) supplemented with 2% (v/v) heat-inactivated bovine serum (Gibco). Human cord blood derived $CD34^+$ HSPCs were purchased from AllCells. Cell number and viability were assessed with a hemocytometer based on trypan blue exclusion.

METHOD DETAILS

pIpC treatment—Expression of Mx1-*Cre* was induced by six intraperitoneal injections of 10mg polyinosinicpolycytidylic acid (pIpC; GE Healthcare) administered every other day, beginning at approximately 6–8 weeks of age.

Flow cytometry and cell sorting—For flow cytometric analysis and isolation of specific hematopoietic mouse progenitors, cells were incubated with combinations of antibodies to the following cell-surface markers, conjugated to FITC, PE, PerCP-Cy5.5, APC, PE-Cy7, eFluor 660, Alexa Fluor 700, APC-eFluor 780 or biotin (clones are given in brackets in the following list): CD3ε (17A2), CD4 (GK1.5), CD5 (53-7.3), CD8α (53-6.7), CD11b (M1/70), CD16/32 (FcγRII/III; 93), CD34 (RAM34), CD41 (MWReg30), CD43 (R2/60), CD45.1 (A20), CD45.2 (104), CD45R (B220; RA3-6B2), CD48 (HM48-1), CD71 (R17217), CD117 (cKit; 2B8), CD127 (IL7Rα; A7R34), CD150 (TC15-12F12.2), Ter119 (TER-119), Sca-1 (D7, E13-161.7), Gr-1 (RB6-8C5) and IgM (II/41). For isolation of HSCs and MPPs, Lineage markers included CD3, CD5, CD8, B220, Gr-1 and Ter119. For isolation of mouse CMPs, GMPs and MEPs, these Lineage markers were supplemented with additional antibodies against CD4 and CD11b. Biotinylated antibodies were visualized by incubation with PE-Cy7 conjugated streptavidin. For analysis of human cord blood derived stem and progenitor cells the APC conjugated anti human CD34 (4H11) was used. All reagents were acquired from eBiosciences, or BioLegend. All incubations were for 30–90 min on ice.

Mouse HSCs, $CD34^+CD16/32^{low}CD127^-Lineage^-Sca\text{-}1^-c\text{-}kit^+$ CMPs (Akashi et al., 2000), $CD34^+CD16/32^{high}CD127^-Lineage^-Sca\text{-}1^-c\text{-}kit^+$ GMPs (Akashi et al., 2000), and $CD34^-CD16/32^{-/low}CD127^-Lineage^-Sca\text{-}1^-c\text{-}kit^+$ MEPs (Akashi et al., 2000) were pre-enriched by selecting $c\text{-}kit^+$ cells using paramagnetic microbeads and an autoMACS magnetic separator (Miltenyi Biotec) before sorting. Non-viable cells were excluded from sorts and analyses using 4',6-diamidino-2-phenylindole (DAPI).

Data acquisition and cell sorting were performed on a FACSAria II, LSR II or FACSCanto flow cytometer (BD Biosciences). Data were analyzed by FlowJo (BD) software.

Ex vivo HSC cultures—$CD150^+CD48^-$LSK HSCs were sorted from the bone marrow of young adult mice directly into 96-well v-bottom plates at a density of 10 cells/well containing freshly made basic HSC culture medium (Prime-XV Mouse Hematopoietic Cell Medium (Prototype; Irvine Scientific) with SCF (50ng/ml; PeproTech), TPO (50ng/ml; PeproTech), 2-Mercaptoethanol (50μM; Sigma) and bovine serum albumin (BSA; 0.1%; Sigma). When specified, basic HSC medium was supplemented with 17-AAG (5nM;

SelleckChem) or HSF1A (8μM, Axon MedChem) in 0.02% DMSO (Sigma). As a control, basic HSC medium was supplemented with 0.02% DMSO.

Human cord blood derived $CD34^+$ HSPCs were cultured in StemSpan (STEMCELL Technologies) with SCF (50ng/ml), Fms-related tyrosine kinase 3 ligand (Flt3-l, 100ng/ml), TPO (100ng/ml; all from PeproTech), 2-Mercaptoethanol (50μM) and BSA (0.1%). HSPC numbers and viability were assessed with a hemocytometer based on trypan blue (Corning) exclusion immediately after thawing. HSPCs were plated into a round-bottom 96-well plate at a density of 2000 cells/well.

Cells were grown in standard cell culture conditions (37°C in 5% CO_2 and air and constant humidity) without any medium change or passaging. After 10d, the entire contents of each individual well were collected and transferred into separate 1.5ml tubes. Wells were also washed 1–2 times to ensure recouping the maximum number of cells. Cells were washed, centrifuged and the supernatant was discarded. Cells were resuspended with 2×10^5 freshly isolated congenic bone marrow cells (unless described otherwise) prior to transplantation.

For assessing the effect of PVA on protein synthesis, HSCs were cultured in F12 medium (Life Technologies) with SCF (10ng/ml), TPO (100ng/ml), Insulin-Transferrin-Selenium-Ethanolamine (ITSX; 1%; Life Technologies), HEPES (10mM; Life Technologies), penicillin/streptomycin/glutamine (1%; Sigma), 2-Mercaptoethanol (50μM) and supplemented with BSA (0.1%) or PVA (0.1%; Sigma) (Wilkinson et al., 2019).

Transplantation assays—Adult recipient mice were administered a minimum lethal dose of radiation using a Mark I Cesium source irradiator (J.L. Sheperd) to deliver two doses of 550 rad (1,100 rad in total) at least 4h apart. Cells were injected into the retro-orbital venous sinus of anaesthetized recipients. For fresh HSC transplants, 10 freshly isolated donor $CD150^+CD48^-$LSK HSCs and 2×10^5 recipient-type bone marrow cells were transplanted. For bone marrow transplants, 5×10^5 unfractionated donor bone marrow cells were transplanted with 5×10^5 recipient-type bone marrow cells. Blood was obtained from the tail veins of recipient mice every 4 weeks for at least 16 weeks after transplantation. Red blood cells were lysed with ammonium chloride potassium buffer. The remaining cells were stained with antibodies against CD45.2, CD45.1, CD45R (B220), CD11b, CD3 and Gr-1 to assess donor-cell engraftment.

For secondary transplants, 3×10^6 bone marrow cells collected from primary recipients were transplanted non-competitively into irradiated recipient mice. Primary recipients used for secondary transplantation had long-term multilineage reconstitution by donor cells and median levels of donor-cell reconstitution for the treatments from which they originated. Mice that died over the course of transplantation experiments were omitted from the analyses. Transplanted mice were administered drinking water with Baytril (250mg/l) for the first 4 weeks post-transplant. Mice were considered long-term multilineage reconstituted if they exhibited >0.5% donor derived peripheral blood B-, T- and myeloid cells 16 weeks post-transplant.

For homing experiments, 3×10^5 LSK cells were transplanted into irradiated recipients. Donor-derived cells were quantified in the bone marrow 24h later.

Limiting dilution assay—For limiting dilution assays, 100, 250, 500, 1000, 3000, 5000 and 10000 cultured cells were aliquoted and transplanted into irradiated recipient mice, together with 2×10^5 recipient-type bone-marrow cells. Limiting dilution analysis was performed using ELDASoftware (Hu and Smyth, 2009). Mice were considered long-term multilineage reconstituted if they exhibited >0.5% donor derived peripheral blood B-, T- and myeloid cells 12 weeks post-transplant.

Colony forming assays—Colony forming units were assessed by plating 5×10^4 unfractionated bone marrow cells in a 3cm petri dish containing methylcellulose culture medium (M3434; STEMCELL Technologies). Cells were grown in standard cell culture conditions (37°C in 5% CO_2 and air and constant humidity) in humidification dishes. Colonies were counted after 14 days.

Immunostaining—For analysis of Hsf1, freshly isolated or cultured HSCs were fixed in 4% paraformaldehyde in PBS for 20 minutes at room temperature. Cells were washed once with PBS then permeabilized with PBS supplemented with 0.1% Triton X-100 (Calbiochem), 0.03% Tween 20 (Sigma) and 1% BSA for 15 minutes at room temperature. Cells were washed three times with PBS supplemented with 0.03% Tween 20. Cells were blocked with PBS supplemented with 1% BSA and 0.03% Tween 20 for 60 minutes at room temperature. Samples were incubated with anti-Hsf1 antibody (Cell Signaling, Rabbit polyclonal (4356), dilution 1:500) overnight at 4°C. Cells were washed three times and incubated with Alexa 488 conjugated anti-Rabbit secondary antibody (A21206; 1:500) for 60 minutes at room temperature. Cells were washed five times with PBS. Before the last wash, nuclei were stained with DAPI for 5 minutes at room temperature. Cells were transferred onto microscope slides and mounted with Vectashield (Vector Laboratories). Images of samples were acquired with a Keyence Microscope and fluorescence intensity was quantified using ImageJ.

Measurement of protein synthesis and proteasome activity—For in vivo analysis, OP-Puro (Medchem Source; 50 mg/kg body mass; pH 6.4–6.6 in PBS) was injected intraperitoneally. One hour later mice were euthanized. Bone marrow was collected, and 4×10^6 cells were stained with combinations of antibodies against cell-surface markers as described above. After washing, cells were fixed in 0.5 ml of 1% paraformaldehyde (Affymetrix) in PBS for 10–15 min on ice. Cells were washed in PBS, then permeabilized in 200 ml PBS supplemented with 3% (v/v) fetal bovine serum (Life Technologies) and 0.1% (m/v) saponin (Sigma) for 5 min at room temperature (20–25°C). The azide-alkyne cycloaddition was performed using the Click-iT Cell Reaction Buffer Kit (Life Technologies) and azide conjugated to Alexa Fluor 555 (Life Technologies) at 5 mM final concentration. After the 30-min reaction, the cells were washed twice in PBS supplemented with 3% fetal bovine serum and 0.1% saponin, then resuspended in PBS supplemented with DAPI (4 mg/ml final concentration) and analyzed by flow cytometry (Hidalgo San Jose and Signer, 2019).

For in vitro analysis, OP-Puro was added to cultured cells at a final concentration of 50 μM for 1 hour. Cells were then collected, washed, fixed and permeabilized prior to performing the azide-alkyne cycloaddition as described above. In some experiments, relative rates of protein synthesis were calculated by normalizing OP-Puro signals in specific populations to unfractionated bone marrow after subtracting background.

Proteasome activity was assessed using the Proteasome-Glo chymotrypsin-like cell based assay (Promega) as previously described (Hidalgo San Jose et al., 2020). GFP expression in UB^{G76V}-*GFP* was analyzed by flow cytometry before or after ex vivo culture.

RNA-sequencing—For RNA-sequencing analysis, total RNA was extracted from ~3000 freshly isolated or cultured HSCs using the RNeasy Plus Micro Kit (Qiagen). Illumina mRNA libraries were prepared using the SMARTseq2 protocol (Picelli et al., 2014). 2.6μl of total RNA was used in the SMARTSeq2 protocol (70pg to 1.62ng). 18 cycles of PCR were performed for the cDNA preamplification step and 12 cycles were performed for the tagmentation library preparation. The resulting libraries were pooled and deep sequenced in two lanes on the Illumina HiSeq 2500 in high output mode using single-end reads with lengths of 50 nucleotides (25–35M reads per condition; Fig. 1) or on the Illumina NovaSeq using paired-end reads with both forward and reverse read lengths of 50 nucleotides (60–100M reads per condition; Fig. 6). The reads that passed Illumina filters were filtered for reads aligning to tRNA, rRNA, adapter sequences, and spike-in controls. The reads were then aligned to the mm10 reference genome using TopHat (v 1.4.1) (Trapnell et al., 2009) (Fig. 1) or GRCm38 reference genome using STAR (v2.6.1) (Dobin et al., 2013) (Fig. 6). DUST scores were calculated with PRINSEQ Lite (v 0.20.3) (Schmieder and Edwards, 2011) and low-complexity reads (DUST > 4) were removed from the BAM files. The alignment results were parsed via the SAMtools (Li et al., 2009) to generate SAM files. Read counts to each genomic feature were obtained with the htseq-count program (v 0.7.1) (Anders et al., 2015) using the “union” option (Fig. 1) or the featureCounts program (v 1.6.5) (Liao et al., 2014) using the default options along with a minimum quality cut off (Phred > 10; Fig. 6). After removing absent features (zero counts in all samples), the raw counts were then imported to Bioconductor package DESeq2 (v 1.24.0) (Love et al., 2014) to identify differentially expressed genes among samples. P-values for differential expression are calculated using the Wald test for differences between the base means of two conditions. These P-values are then adjusted for multiple test correction using Benjamini Hochberg algorithm. We considered genes differentially expressed between two groups of samples when the DESeq2 analysis resulted in an adjusted P-value of <0.05 and the difference in gene expression was at least 2-fold (Fig. 1) or 1.5-fold (Fig. 6).

Previously published RNA-sequencing data for young and old HSCs (Young et al., 2021) were compared to the 55 significantly upregulated genes that were associated with Hsf1 activation (Table S3). Gene counts produced by RSEM were obtained from GEO and then imported to Bioconductor package DESeq2 (v1.30.1) (Love et al., 2014) to identify differentially expressed genes among samples. A binomial assignment of upregulated or downregulated was made without any threshold cutoffs.

QUANTIFICATION AND STATISTICAL ANALYSIS

Group data are represented by mean ± standard deviation (SD) or standard error of the mean (SEM), as specified in figure legends. To test statistical significance between two samples, two-tailed Student's t-tests were typically used. We also used Student's t-tests, rather than an ANOVA to compare both 17-AAG and HSF1A to DMSO, based on our pre-established hypothesis about the independent nature of these treatments (i.e. the null hypothesis was that 17-AAG = DMSO or HSF1A = DMSO). In most cases where the Student's t-tests were statistically significant, the ANOVA was also statistically significant. Statistical significance comparing overall numbers of mice with long-term multilineage reconstitution was assessed by a Fisher's exact test. The specific type of test used for each figure panel is described in the figure legends.

For normalized data, means were calculated and statistical tests were performed using log10-transformed data and then means were back-transformed to prevent data skewing. No randomization or blinding was used in any experiments. The only mice excluded from any experiment were those that died after transplantation. Transplantation experiments were excluded when >50% of mice died.

In the case of measurements in which variation among experiments tends to be low (for example, HSC frequency) we generally examined 3 to 6 mice. In the case of measurements in which variation among experiments tends to be higher (for example, reconstitution assays) we examined larger numbers of mice (>10). We performed multiple independent experiments with multiple biological replicates to ensure the reproducibility of our findings.

Supplementary Material

Refer to Web version on PubMed Central for supplementary material.

Acknowledgements

Work in the Signer Laboratory is supported by the NIH/NIDDK (R01DK116951; R01DK124775), and the Blood Cancer Discoveries Grant program (8025-20) through The Leukemia & Lymphoma Society, The Mark Foundation for Cancer Research and The Paul G. Allen Frontiers Group, Scholar Awards from the V Foundation for Cancer Research (V2017-003) and the American Society of Hematology, the Sanford Stem Cell Clinical Center, and the UC San Diego Moores Cancer Center which is supported by the NCI Cancer Center Support Grant (P30CA023100). The LJI Flow Cytometry core facility is supported by the NIH Shared Instrumentation Grant Program (S10 RR027366). The graphical abstract was created with BioRender.com. We would like to thank E. Christians for the *Hsf1*^{fl} mice, J. Magee, S. Morrison, K. Dorshkind and J. Vincent for advice.

REFERENCES

Abbas HA, Maccio DR, Coskun S, Jackson JG, Hazen AL, Sills TM, You MJ, Hirschi KK, and Lozano G (2010). Mdm2 is required for survival of hematopoietic stem cells/progenitors via dampening of ROS-induced p53 activity. Cell stem cell 7, 606–617. [PubMed: 21040902]

Akashi K, Traver D, Miyamoto T, and Weissman IL (2000). A clonogenic common myeloid progenitor that gives rise to all myeloid lineages. Nature 404, 193–197. [PubMed: 10724173]

Akerfelt M, Morimoto RI, and Sistonen L (2010). Heat shock factors: integrators of cell stress, development and lifespan. Nat Rev Mol Cell Biol 11, 545–555. [PubMed: 20628411]

Allsopp RC, Cheshier S, and Weissman IL (2001). Telomere shortening accompanies increased cell cycle activity during serial transplantation of hematopoietic stem cells. The Journal of experimental medicine 193, 917–924. [PubMed: 11304552]

Alvarez S, Diaz M, Flach J, Rodriguez-Acebes S, Lopez-Contreras AJ, Martinez D, Canamero M, Fernandez-Capetillo O, Isern J, Passegue E, et al. (2015). Replication stress caused by low MCM expression limits fetal erythropoiesis and hematopoietic stem cell functionality. Nat Commun 6, 8548. [PubMed: 26456157]

Anckar J, and Sistonen L (2011). Regulation of HSF1 function in the heat stress response: implications in aging and disease. Annu Rev Biochem 80, 1089–1115. [PubMed: 21417720]

Baird NA, Douglas PM, Simic MS, Grant AR, Moresco JJ, Wolff SC, Yates JR 3rd, Manning G, and Dillin A (2014). HSF-1-mediated cytoskeletal integrity determines thermotolerance and life span. Science 346, 360–363. [PubMed: 25324391]

Beerman I, Seita J, Inlay MA, Weissman IL, and Rossi DJ (2014). Quiescent hematopoietic stem cells accumulate DNA damage during aging that is repaired upon entry into cell cycle. Cell stem cell 15, 37–50. [PubMed: 24813857]

Boitano AE, Wang J, Romeo R, Bouchez LC, Parker AE, Sutton SE, Walker JR, Flaveny CA, Perdew GH, Denison MS, et al. (2010). Aryl hydrocarbon receptor antagonists promote the expansion of human hematopoietic stem cells. Science 329, 1345–1348. [PubMed: 20688981]

Bowman TV, and Zon LI (2009). Lessons from the Niche for Generation and Expansion of Hematopoietic Stem Cells. Drug Discov Today Ther Strateg 6, 135–140. [PubMed: 21212834]

Buszczak M, Signer RA, and Morrison SJ (2014). Cellular differences in protein synthesis regulate tissue homeostasis. Cell 159, 242–251. [PubMed: 25303523]

Calvanese V, Nguyen AT, Bolan TJ, Vavilina A, Su T, Lee LK, Wang Y, Lay FD, Magnusson M, Crooks GM, et al. (2019). MLLT3 governs human haematopoietic stem-cell self-renewal and engraftment. Nature 576, 281–286. [PubMed: 31776511]

Chambers SM, Shaw CA, Gatza C, Fisk CJ, Donehower LA, and Goodell MA (2007). Aging hematopoietic stem cells decline in function and exhibit epigenetic dysregulation. PLoS Biol 5, e201. [PubMed: 17676974]

Cheshier SH, Morrison SJ, Liao X, and Weissman IL (1999). In vivo proliferation and cell cycle kinetics of long-term self-renewing hematopoietic stem cells. Proceedings of the National Academy of Sciences of the United States of America 96, 3120–3125. [PubMed: 10077647]

Chua BA, and Signer RAJ (2020). Hematopoietic stem cell regulation by the proteostasis network. Curr Opin Hematol 27, 254–263. [PubMed: 32452878]

Chua BA, Van Der Werf I, Jamieson C, and Signer RAJ (2020). Post-Transcriptional Regulation of Homeostatic, Stressed, and Malignant Stem Cells. Cell stem cell 26, 138–159. [PubMed: 32032524]

Ciechanover A, and Kwon YT (2015). Degradation of misfolded proteins in neurodegenerative diseases: therapeutic targets and strategies. Exp Mol Med 47, e147. [PubMed: 25766616]

Copelan EA (2006). Hematopoietic stem-cell transplantation. N Engl J Med 354, 1813–1826. [PubMed: 16641398]

Crane GM, Jeffery E, and Morrison SJ (2017). Adult haematopoietic stem cell niches. Nat Rev Immunol 17, 573–590. [PubMed: 28604734]

Dobin A, Davis CA, Schlesinger F, Drenkow J, Zaleski C, Jha S, Batut P, Chaisson M, and Gingeras TR (2013). STAR: ultrafast universal RNA-seq aligner. Bioinformatics 29, 15–21. [PubMed: 23104886]

Eliasson P, Rehn M, Hammar P, Larsson P, Sirenko O, Flippin LA, Cammenga J, and Jonsson JI (2010). Hypoxia mediates low cell-cycle activity and increases the proportion of long-term-reconstituting hematopoietic stem cells during in vitro culture. Experimental hematology 38, 301–310 e302. [PubMed: 20138114]

Essers MA, Offner S, Blanco-Bose WE, Waibler Z, Kalinke U, Duchosal MA, and Trumpp A (2009). IFNalpha activates dormant haematopoietic stem cells in vivo. Nature 458, 904–908. [PubMed: 19212321]

Fares I, Chagraoui J, Gareau Y, Gingras S, Ruel R, Mayotte N, Csaszar E, Knapp DJ, Miller P, Ngom M, et al. (2014). Cord blood expansion. Pyrimidoindole derivatives are agonists of human hematopoietic stem cell self-renewal. Science 345, 1509–1512. [PubMed: 25237102]

Flach J, Bakker ST, Mohrin M, Conroy PC, Pietras EM, Reynaud D, Alvarez S, Diolaiti ME, Ugarte F, Forsberg EC, et al. (2014). Replication stress is a potent driver of functional decline in ageing haematopoietic stem cells. Nature 512, 198–202. [PubMed: 25079315]

Gan B, Hu J, Jiang S, Liu Y, Sahin E, Zhuang L, Fletcher-Sananikone E, Colla S, Wang YA, Chin L, et al. (2010). Lkb1 regulates quiescence and metabolic homeostasis of haematopoietic stem cells. Nature 468, 701–704. [PubMed: 21124456]

Guo B, Huang X, Lee MR, Lee SA, and Broxmeyer HE (2018). Antagonism of PPAR-gamma signaling expands human hematopoietic stem and progenitor cells by enhancing glycolysis. Nat Med 24, 360–367. [PubMed: 29377004]

Gurumurthy S, Xie SZ, Alagesan B, Kim J, Yusuf RZ, Saez B, Tzatsos A, Ozsolak F, Milos P, Ferrari F, et al. (2010). The Lkb1 metabolic sensor maintains haematopoietic stem cell survival. Nature 468, 659–663. [PubMed: 21124451]

Hidalgo San Jose L, and Signer RAJ (2019). Cell-type-specific quantification of protein synthesis in vivo. Nat Protoc 14, 441–460. [PubMed: 30610239]

Hidalgo San Jose L, Sunshine MJ, Dillingham CH, Chua BA, Kruta M, Hong Y, Hatters DM, and Signer RAJ (2020). Modest Declines in Proteome Quality Impair Hematopoietic Stem Cell Self-Renewal. Cell Rep 30, 69–80 e66. [PubMed: 31914399]

Hipp MS, Kasturi P, and Hartl FU (2019). The proteostasis network and its decline in ageing. Nat Rev Mol Cell Biol 20, 421–435. [PubMed: 30733602]

Ho TT, Warr MR, Adelman ER, Lansinger OM, Flach J, Verovskaya EV, Figueroa ME, and Passegue E (2017). Autophagy maintains the metabolism and function of young and old stem cells. Nature 543, 205–210. [PubMed: 28241143]

Hu Y, and Smyth GK (2009). ELDA: extreme limiting dilution analysis for comparing depleted and enriched populations in stem cell and other assays. J Immunol Methods 347, 70–78. [PubMed: 19567251]

Huang J, Nguyen-McCarty M, Hexner EO, Danet-Desnoyers G, and Klein PS (2012). Maintenance of hematopoietic stem cells through regulation of Wnt and mTOR pathways. Nat Med 18, 1778–1785. [PubMed: 23142822]

Ito K, Hirao A, Arai F, Matsuoka S, Takubo K, Hamaguchi I, Nomiyama K, Hosokawa K, Sakurada K, Nakagata N, et al. (2004). Regulation of oxidative stress by ATM is required for self-renewal of haematopoietic stem cells. Nature 431, 997–1002. [PubMed: 15496926]

Ito K, Hirao A, Arai F, Takubo K, Matsuoka S, Miyamoto K, Ohmura M, Naka K, Hosokawa K, Ikeda Y, et al. (2006). Reactive oxygen species act through p38 MAPK to limit the lifespan of hematopoietic stem cells. Nat Med 12, 446–451. [PubMed: 16565722]

Janzen V, Forkert R, Fleming HE, Saito Y, Waring MT, Dombkowski DM, Cheng T, DePinho RA, Sharpless NE, and Scadden DT (2006). Stem-cell ageing modified by the cyclin-dependent kinase inhibitor p16INK4a. Nature 443, 421–426. [PubMed: 16957735]

Karigane D, Kobayashi H, Morikawa T, Ootomo Y, Sakai M, Nagamatsu G, Kubota Y, Goda N, Matsumoto M, Nishimura EK, et al. (2016). p38alpha Activates Purine Metabolism to Initiate Hematopoietic Stem/Progenitor Cell Cycling in Response to Stress. Cell stem cell 19, 192–204. [PubMed: 27345838]

Kiel MJ, Yilmaz OH, Iwashita T, Yilmaz OH, Terhorst C, and Morrison SJ (2005). SLAM family receptors distinguish hematopoietic stem and progenitor cells and reveal endothelial niches for stem cells. Cell 121, 1109–1121. [PubMed: 15989959]

Kourtis N, Lazaris C, Hockemeyer K, Balandran JC, Jimenez AR, Mullenders J, Gong Y, Trimarchi T, Bhatt K, Hu H, et al. (2018). Oncogenic hijacking of the stress response machinery in T cell acute lymphoblastic leukemia. Nat Med 24, 1157–1166. [PubMed: 30038221]

Kovacs D, Sigmond T, Hotzi B, Bohar B, Fazekas D, Deak V, Vellai T, and Barna J (2019). HSF1Base: A Comprehensive Database of HSF1 (Heat Shock Factor 1) Target Genes. Int J Mol Sci 20.

Kuhn R, Schwenk F, Aguet M, and Rajewsky K (1995). Inducible gene targeting in mice. Science 269, 1427–1429. [PubMed: 7660125]

Kumar S, and Geiger H (2017). HSC Niche Biology and HSC Expansion Ex Vivo. Trends Mol Med 23, 799–819. [PubMed: 28801069]

Kundra R, Ciryam P, Morimoto RI, Dobson CM, and Vendruscolo M (2017). Protein homeostasis of a metastable subproteome associated with Alzheimer's disease. Proceedings of the National Academy of Sciences of the United States of America 114, E5703–E5711. [PubMed: 28652376]

Le Masson F, Razak Z, Kaigo M, Audouard C, Charry C, Cooke H, Westwood JT, and Christians ES (2011). Identification of heat shock factor 1 molecular and cellular targets during embryonic and adult female meiosis. Mol Cell Biol 31, 3410–3423. [PubMed: 21690297]

Li H, Handsaker B, Wysoker A, Fennell T, Ruan J, Homer N, Marth G, Abecasis G, Durbin R, and Genome Project Data Processing, S. (2009). The Sequence Alignment/Map format and SAMtools. Bioinformatics 25, 2078–2079. [PubMed: 19505943]

Li J, Labbadia J, and Morimoto RI (2017). Rethinking HSF1 in Stress, Development, and Organismal Health. Trends Cell Biol 27, 895–905. [PubMed: 28890254]

Liao Y, Smyth GK, and Shi W (2014). featureCounts: an efficient general purpose program for assigning sequence reads to genomic features. Bioinformatics 30, 923–930. [PubMed: 24227677]

Lindquist S (1981). Regulation of protein synthesis during heat shock. Nature 293, 311–314. [PubMed: 6792546]

Lindsten K, Menendez-Benito V, Masucci MG, and Dantuma NP (2003). A transgenic mouse model of the ubiquitin/proteasome system. Nat Biotechnol 21, 897–902. [PubMed: 12872133]

Liu J, Xu Y, Stoleru D, and Salic A (2012). Imaging protein synthesis in cells and tissues with an alkyne analog of puromycin. Proceedings of the National Academy of Sciences of the United States of America 109, 413–418. [PubMed: 22160674]

Liu X, Zheng H, Yu WM, Cooper TM, Bunting KD, and Qu CK (2015). Maintenance of mouse hematopoietic stem cells ex vivo by reprogramming cellular metabolism. Blood 125, 1562–1565. [PubMed: 25593337]

Lopez-Otin C, Blasco MA, Partridge L, Serrano M, and Kroemer G (2013). The hallmarks of aging. Cell 153, 1194–1217. [PubMed: 23746838]

Love MI, Huber W, and Anders S (2014). Moderated estimation of fold change and dispersion for RNA-seq data with DESeq2. Genome Biol 15, 550. [PubMed: 25516281]

Luchsinger LL, Strikoudis A, Danzl NM, Bush EC, Finlayson MO, Satwani P, Sykes M, Yazawa M, and Snoeck HW (2019). Harnessing Hematopoietic Stem Cell Low Intracellular Calcium Improves Their Maintenance In Vitro. Cell stem cell 25, 225–240 e227. [PubMed: 31178255]

Magee JA, and Signer RAJ (2021). Developmental Stage-Specific Changes in Protein Synthesis Differentially Sensitize Hematopoietic Stem Cells and Erythroid Progenitors to Impaired Ribosome Biogenesis. Stem Cell Reports 16, 20–28. [PubMed: 33440178]

Mansell E, Sigurdsson V, Deltcheva E, Brown J, James C, Miharada K, Soneji S, Larsson J, and Enver T (2021). Mitochondrial Potentiation Ameliorates Age-Related Heterogeneity in Hematopoietic Stem Cell Function. Cell stem cell 28, 241–256 e246. [PubMed: 33086034]

Mantel CR, O'Leary HA, Chitteti BR, Huang X, Cooper S, Hangoc G, Brustovetsky N, Srour EF, Lee MR, Messina-Graham S, et al. (2015). Enhancing Hematopoietic Stem Cell Transplantation Efficacy by Mitigating Oxygen Shock. Cell 161, 1553–1565. [PubMed: 26073944]

Maryanovich M, Zaltsman Y, Ruggiero A, Goldman A, Shachnai L, Zaidman SL, Porat Z, Golan K, Lapidot T, and Gross A (2015). An MTCH2 pathway repressing mitochondria metabolism regulates haematopoietic stem cell fate. Nat Commun 6, 7901. [PubMed: 26219591]

Mendillo ML, Santagata S, Koeva M, Bell GW, Hu R, Tamimi RM, Fraenkel E, Ince TA, Whitesell L, and Lindquist S (2012). HSF1 drives a transcriptional program distinct from heat shock to support highly malignant human cancers. Cell 150, 549–562. [PubMed: 22863008]

Miharada K, Sigurdsson V, and Karlsson S (2014). Dppa5 improves hematopoietic stem cell activity by reducing endoplasmic reticulum stress. Cell Rep 7, 1381–1392. [PubMed: 24882002]

Milyavsky M, Gan OI, Trottier M, Komosa M, Tabach O, Notta F, Lechman E, Hermans KG, Eppert K, Konovalova Z, et al. (2010). A distinctive DNA damage response in human hematopoietic stem cells reveals an apoptosis-independent role for p53 in self-renewal. Cell stem cell 7, 186–197. [PubMed: 20619763]

Mohrin M, Bourke E, Alexander D, Warr MR, Barry-Holson K, Le Beau MM, Morrison CG, and Passegue E (2010). Hematopoietic stem cell quiescence promotes error-prone DNA repair and mutagenesis. Cell stem cell 7, 174–185. [PubMed: 20619762]

Mohrin M, Shin J, Liu Y, Brown K, Luo H, Xi Y, Haynes CM, and Chen D (2015). Stem cell aging. A mitochondrial UPR-mediated metabolic checkpoint regulates hematopoietic stem cell aging. Science 347, 1374–1377. [PubMed: 25792330]

Morrison SJ, Wright DE, and Weissman IL (1997). Cyclophosphamide/granulocyte colony-stimulating factor induces hematopoietic stem cells to proliferate prior to mobilization. Proceedings of the National Academy of Sciences of the United States of America 94, 1908–1913. [PubMed: 9050878]

Nakada D, Saunders TL, and Morrison SJ (2010). Lkb1 regulates cell cycle and energy metabolism in haematopoietic stem cells. Nature 468, 653–658. [PubMed: 21124450]

Naldini L (2015). Gene therapy returns to centre stage. Nature 526, 351–360. [PubMed: 26469046]

Neef DW, Jaeger AM, Gomez-Pastor R, Willmund F, Frydman J, and Thiele DJ (2014). A direct regulatory interaction between chaperonin TRiC and stress-responsive transcription factor HSF1. Cell Rep 9, 955–966. [PubMed: 25437552]

Neef DW, Turski ML, and Thiele DJ (2010). Modulation of heat shock transcription factor 1 as a therapeutic target for small molecule intervention in neurodegenerative disease. PLoS Biol 8, e1000291. [PubMed: 20098725]

Olson OC, Kang YA, and Passegue E (2020). Normal Hematopoiesis Is a Balancing Act of Self-Renewal and Regeneration. Cold Spring Harb Perspect Med.

Picelli S, Faridani OR, Bjorklund AK, Winberg G, Sagasser S, and Sandberg R (2014). Full-length RNA-seq from single cells using Smart-seq2. Nat Protoc 9, 171–181. [PubMed: 24385147]

Pietras EM (2017). Inflammation: a key regulator of hematopoietic stem cell fate in health and disease. Blood 130, 1693–1698. [PubMed: 28874349]

Purton LE, and Scadden DT (2007). Limiting factors in murine hematopoietic stem cell assays. Cell stem cell 1, 263–270. [PubMed: 18371361]

Ray PD, Huang BW, and Tsuji Y (2012). Reactive oxygen species (ROS) homeostasis and redox regulation in cellular signaling. Cell Signal 24, 981–990. [PubMed: 22286106]

Rossi DJ, Bryder D, Seita J, Nussenzweig A, Hoeijmakers J, and Weissman IL (2007). Deficiencies in DNA damage repair limit the function of haematopoietic stem cells with age. Nature 447, 725–729. [PubMed: 17554309]

Rossin F, Villella VR, D'Eletto M, Farrace MG, Esposito S, Ferrari E, Monzani R, Occhigrossi L, Pagliarini V, Sette C, et al. (2018). TG2 regulates the heat-shock response by the post-translational modification of HSF1. EMBO Rep 19.

Schmieder R, and Edwards R (2011). Quality control and preprocessing of metagenomic datasets. Bioinformatics 27, 863–864. [PubMed: 21278185]

Schulte TW, and Neckers LM (1998). The benzoquinone ansamycin 17-allylamino-17-demethoxygeldanamycin binds to HSP90 and shares important biologic activities with geldanamycin. Cancer Chemother Pharmacol 42, 273–279. [PubMed: 9744771]

Shi Y, Mosser DD, and Morimoto RI (1998). Molecular chaperones as HSF1-specific transcriptional repressors. Genes Dev 12, 654–666. [PubMed: 9499401]

Signer RA, Magee JA, Salic A, and Morrison SJ (2014). Haematopoietic stem cells require a highly regulated protein synthesis rate. Nature 509, 49–54. [PubMed: 24670665]

Signer RA, Qi L, Zhao Z, Thompson D, Sigova AA, Fan ZP, DeMartino GN, Young RA, Sonenberg N, and Morrison SJ (2016). The rate of protein synthesis in hematopoietic stem cells is limited partly by 4E-BPs. Genes Dev 30, 1698–1703. [PubMed: 27492367]

Subramanian A, Tamayo P, Mootha VK, Mukherjee S, Ebert BL, Gillette MA, Paulovich A, Pomeroy SL, Golub TR, Lander ES, et al. (2005). Gene set enrichment analysis: a knowledge-based approach for interpreting genome-wide expression profiles. Proceedings of the National Academy of Sciences of the United States of America 102, 15545–15550. [PubMed: 16199517]

Sun D, Luo M, Jeong M, Rodriguez B, Xia Z, Hannah R, Wang H, Le T, Faull KF, Chen R, et al. (2014). Epigenomic profiling of young and aged HSCs reveals concerted changes during aging that reinforce self-renewal. Cell stem cell 14, 673–688. [PubMed: 24792119]

Takubo K, Nagamatsu G, Kobayashi CI, Nakamura-Ishizu A, Kobayashi H, Ikeda E, Goda N, Rahimi Y, Johnson RS, Soga T, et al. (2013). Regulation of glycolysis by Pdk functions as a metabolic

checkpoint for cell cycle quiescence in hematopoietic stem cells. Cell stem cell 12, 49–61. [PubMed: 23290136]

Taylor RC, and Dillin A (2011). Aging as an event of proteostasis collapse. Cold Spring Harb Perspect Biol 3.

Tothova Z, Kollipara R, Huntly BJ, Lee BH, Castrillon DH, Cullen DE, McDowell EP, Lazo-Kallanian S, Williams IR, Sears C, et al. (2007). FoxOs are critical mediators of hematopoietic stem cell resistance to physiologic oxidative stress. Cell 128, 325–339. [PubMed: 17254970]

van Galen P, Mbong N, Kreso A, Schoof EM, Wagenblast E, Ng SWK, Krivdova G, Jin L, Nakauchi H, and Dick JE (2018). Integrated Stress Response Activity Marks Stem Cells in Normal Hematopoiesis and Leukemia. Cell Rep 25, 1109–1117 e1105. [PubMed: 30380403]

Walter D, Lier A, Geiselhart A, Thalheimer FB, Huntscha S, Sobotta MC, Moehrle B, Brocks D, Bayindir I, Kaschutnig P, et al. (2015). Exit from dormancy provokes DNA-damage-induced attrition in haematopoietic stem cells. Nature 520, 549–552. [PubMed: 25707806]

Wang J, Sun Q, Morita Y, Jiang H, Gross A, Lechel A, Hildner K, Guachalla LM, Gompf A, Hartmann D, et al. (2012). A differentiation checkpoint limits hematopoietic stem cell self-renewal in response to DNA damage. Cell 148, 1001–1014. [PubMed: 22385964]

Wilkinson AC, Ishida R, Kikuchi M, Sudo K, Morita M, Crisostomo RV, Yamamoto R, Loh KM, Nakamura Y, Watanabe M, et al. (2019). Long-term ex vivo haematopoietic-stem-cell expansion allows nonconditioned transplantation. Nature.

Xiao N, Jani K, Morgan K, Okabe R, Cullen DE, Jesneck JL, and Raffel GD (2012). Hematopoietic stem cells lacking Ott1 display aspects associated with aging and are unable to maintain quiescence during proliferative stress. Blood 119, 4898–4907. [PubMed: 22490678]

Young K, Eudy E, Bell R, Loberg MA, Stearns T, Sharma D, Velten L, Haas S, Filippi MD, and Trowbridge JJ (2021). Decline in IGF1 in the bone marrow microenvironment initiates hematopoietic stem cell aging. Cell stem cell.

Yu WM, Liu X, Shen J, Jovanovic O, Pohl EE, Gerson SL, Finkel T, Broxmeyer HE, and Qu CK (2013). Metabolic regulation by the mitochondrial phosphatase PTPMT1 is required for hematopoietic stem cell differentiation. Cell stem cell 12, 62–74. [PubMed: 23290137]

Zhang CC, and Lodish HF (2005). Murine hematopoietic stem cells change their surface phenotype during ex vivo expansion. Blood 105, 4314–4320. [PubMed: 15701724]

Zou J, Guo Y, Guettouche T, Smith DF, and Voellmy R (1998). Repression of heat shock transcription factor HSF1 activation by HSP90 (HSP90 complex) that forms a stress-sensitive complex with HSF1. Cell 94, 471–480. [PubMed: 9727490]

Highlights

- Ex vivo cultured HSCs rapidly and massively increase protein synthesis
- Hsf1 is activated in culture to promote ex vivo HSC maintenance and proteostasis
- Small molecule activators of Hsf1 enhance HSC maintenance and fitness in culture
- Hsf1 is activated in aging HSCs in vivo to promote proteostasis and fitness

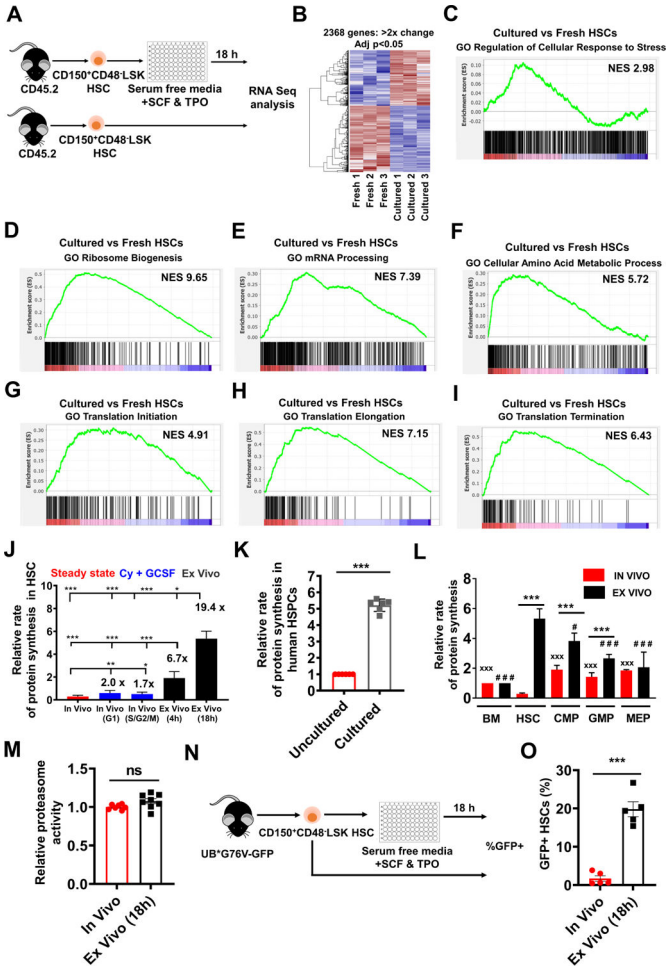

Figure 1. Ex vivo cultured HSCs exhibit increased protein synthesis.

(A) Strategy to compare gene expression in fresh and cultured HSCs. (B) Heat map showing differentially expressed transcripts (≥2-fold change; Padj<0.05) between fresh and cultured (18h) HSCs (n=3). (C-I) Gene set enrichment analysis demonstrating elevated expression of gene sets related to (C) cellular response to stress and (D–I) protein synthesis in cultured compared to fresh HSCs. (J) Protein synthesis in steady state, cycling (G1) and dividing (S/G2/M) HSCs in vivo, and cultured HSCs (4h and 18h). OP-Puro incorporation is normalized to bone marrow cells from identical conditions (n=10 mice for in vivo and n=3 for ex vivo; Cy + GCSF data reanalyzed from (Signer et al., 2014)). (K) Relative protein synthesis in fresh and cultured (18h) human cord blood $CD34^+$ cells (n=6 wells, 2 experiments). (L) Relative protein synthesis in bone marrow cells (BM), HSCs, CMPs, GMPs and MEPs in vivo and after 18h in culture (n=3). (M) Relative proteasome activity in fresh and cultured (18h) $CD48^-$LSK cells (n=7–8/condition in 2 experiments). (N) Strategy to examine proteostasis imbalance within cultured Ub^{G76V}-*GFP* HSCs. (O) Frequency of GFP^+ HSCs in vivo or after culture (18h) of Ub^{G76V}-*GFP* HSCs. Data in J-O represent mean ± SD. Significance in J-O was assessed using a t-test (*P<0.05; **P<0.01; ***P<0.001). In L, xxxP<0.001 relative to HSCs in vivo and ###P<0.001 relative to HSCs ex vivo.

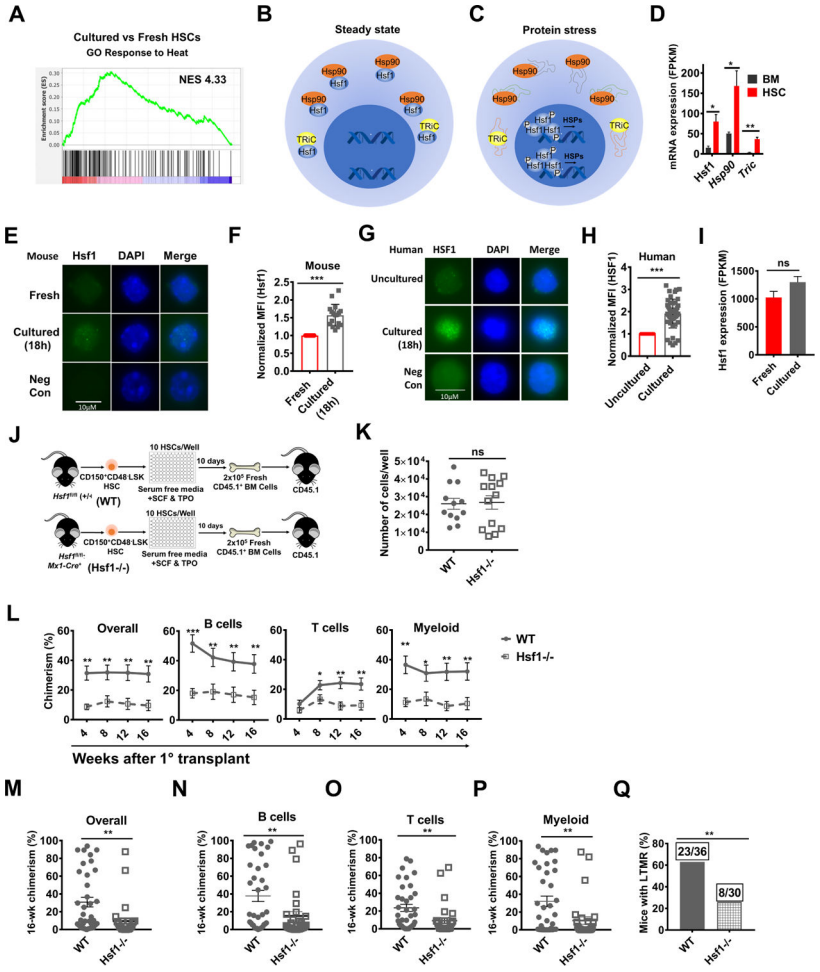

Figure 2. Hsf1 promotes ex vivo HSC maintenance.

(A) Gene set enrichment plot demonstrating elevated expression of the “Response to Heat” gene set in cultured relative to fresh HSCs. (B,C) Diagram showing that at steady state (B), Hsf1 is sequestered in the cytoplasm via binding to chaperones, but under conditions of protein stress (C) chaperones bind unfolded proteins allowing Hsf1 to translocate to the nucleus, where it drives transcription of heat shock proteins (HSPs). (D) *Hsf1*, *Hsp90aa1* (Hsp90) and *Tcp1* (TRiC) expression in HSCs and bone marrow cells (n=3; from dataset in (Signer et al., 2016)). (E,G) Representative immunofluorescence staining examining Hsf1 expression in fresh and 18h cultured (E) mouse HSCs and (G) human cord blood $CD34^+$ cells. Negative control is staining in the absence of primary antibody. (F,H) Quantification of nuclear Hsf1 expression in fresh and 18h cultured (F) mouse HSCs (n=17–21 cells/condition in 2–3 experiments; MFI = mean fluorescence intensity) and (H) human cord blood $CD34^+$ cells (n=45–48 cells/condition in 2 experiments). (I) Hsf1 expression in fresh and cultured (18h) mouse HSCs (n=3). (J) Strategy to compare the long-term reconstituting activity of cultured *Hsf1*$^{fl/fl}$ (WT) and *Hsf1*$^{fl/fl}$;Mx1-*Cre*$^+$ (*Hsf1*$^{-/-}$) HSCs. (K) Number of cells/well from 10d culture of 10 WT and *Hsf1*$^{-/-}$ HSCs (n=12–13 wells/genotype in 2 experiments). (L) Donor cell engraftment when 10 WT or *Hsf1*$^{-/-}$ HSCs were cultured for 10d and transplanted with 2×10^5 recipient-type bone marrow cells into irradiated mice. Total hematopoietic, B-, T- and myeloid cell engraftment are shown (n=6–7 donors, 30–36

recipients/genotype). (M-P) Long-term (16-week) donor (M) hematopoietic, (N) B-, (O) T- and (P) myeloid cell engraftment in the peripheral blood of individual recipients in L. (Q) Frequency of recipients in (L–P) that exhibited long-term (16-week) multilineage reconstitution (LTMR). Data represent mean ± SD (D, F, H, I) or SEM (K-P). Significance was assessed using a t-test (D, F, H, I, K-P) or a Fisher's exact test (Q) (*P<0.05; **P<0.01).

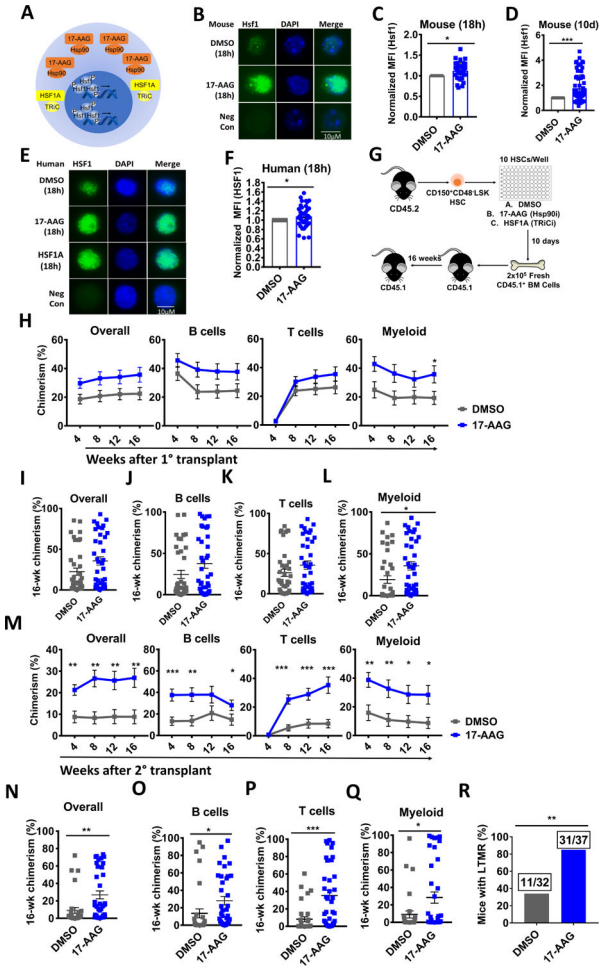

Figure 3. 17-AAG enhances the serial reconstituting activity of ex vivo cultured HSCs

(A) Diagram showing that 17-AAG and HSF1A can promote Hsf1 nuclear localization by inhibiting its interaction with Hsp90 and TRiC. (B,E) Representative immunofluorescence staining examining Hsf1 expression in (B) mouse HSCs or (E) human cord blood CD34$^+$ cells cultured for 18h in basic HSC medium supplemented with DMSO or 17-AAG. Negative control is staining in the absence of primary antibody. (C,D) Quantification of Hsf1 expression in HSCs cultured for (C) 18h or (D) 10d in basic HSC medium supplemented with DMSO or 17-AAG (n=17–109 cells/condition in 3–4 experiments). (F) Quantification of nuclear HSF1 expression in human cord blood CD34$^+$ cells cultured for 18h in basic medium supplemented with DMSO or 17-AAG (n=23–48 cells/condition in 2 experiments). (G) Strategy to compare the effect of 17-AAG and HSF1A on serial reconstituting activity of cultured HSCs. (H) Donor cell engraftment when 10 HSCs were cultured for 10d in basic HSC medium supplemented with DMSO or 17-AAG and transplanted with 2×10^5 recipient-type bone marrow cells into irradiated mice. Total hematopoietic, B-, T- and myeloid cell engraftment are shown (n=6–8 donors, 29–39 recipients/condition). (I-L) Long-term donor (I) hematopoietic, (J) B-, (K) T- and (L) myeloid cell engraftment in the peripheral blood of individual mice from transplants in H. (M) Donor cell engraftment after serial transplantation of 3×10^6 bone marrow cells from primary recipients in H-L into secondary recipients. Total hematopoietic, B-, T- and myeloid cell engraftment are shown (n=7–10

donors, 32–37 recipients/condition). (N-Q) Long-term donor (N) hematopoietic, (O) B-, (P) T- and (Q) myeloid cell engraftment in the peripheral blood of individual recipient mice from transplants in M. (R) Frequency of secondary recipients in (M-R) that exhibited long-term multilineage reconstitution (LTMR). Data represent mean ± SD (C, D, F) or SEM (H-Q). Significance was assessed using a t-test (C, D, F, H-Q) or a Fisher's exact test (R) (*P<0.05; **P<0.01, ***P<0.001 relative to DMSO).

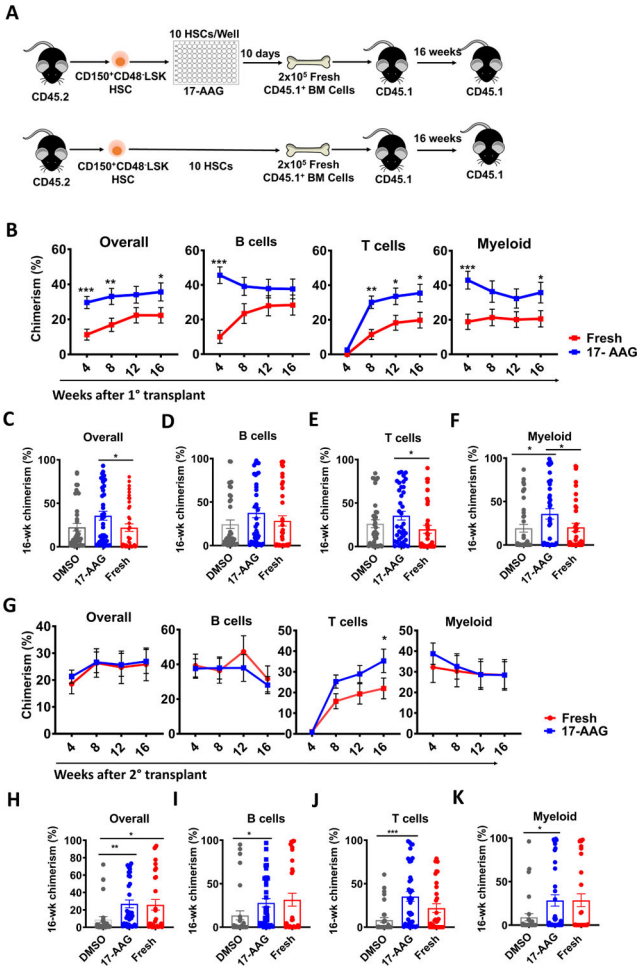

Figure 4. 17-AAG promotes ex vivo maintenance of HSC fitness.

(A) Strategy to compare the serial reconstituting activity of fresh and cultured (17-AAG) HSCs. (B) Donor cell engraftment when 10 fresh or cultured (10d with 17-AAG) HSCs were transplanted with 2×10^5 recipient-type bone marrow cells into irradiated mice. Total hematopoietic, B-, T- and myeloid cell engraftment are shown (n=8–10 donors, 31–39 recipients/condition). (C-F) Long-term donor (C) hematopoietic, (D) B-, (E) T- and (F) myeloid cell engraftment in the peripheral blood of recipient mice from transplants in B (for 17-AAG these are the same mice as shown in Fig. 3E–I). (G) Donor cell engraftment after serial transplantation of 3×10^6 bone marrow cells from primary recipients in C-G into secondary recipients. Total hematopoietic, B-, T- and myeloid cell engraftment are shown (n=7–10 donors, 31–37 total recipients/condition). (H-K) Long-term donor (H) hematopoietic, (I) B-, (J) T- and (K) myeloid cell engraftment in the peripheral blood of individual mice from transplants in F (for 17-AAG these are the same mice as shown in Fig. 3H–R). Data in B-K represent mean ± SEM. Significance was assessed using a t-test (B-K) (*P<0.05; **P<0.01; ***P<0.001).

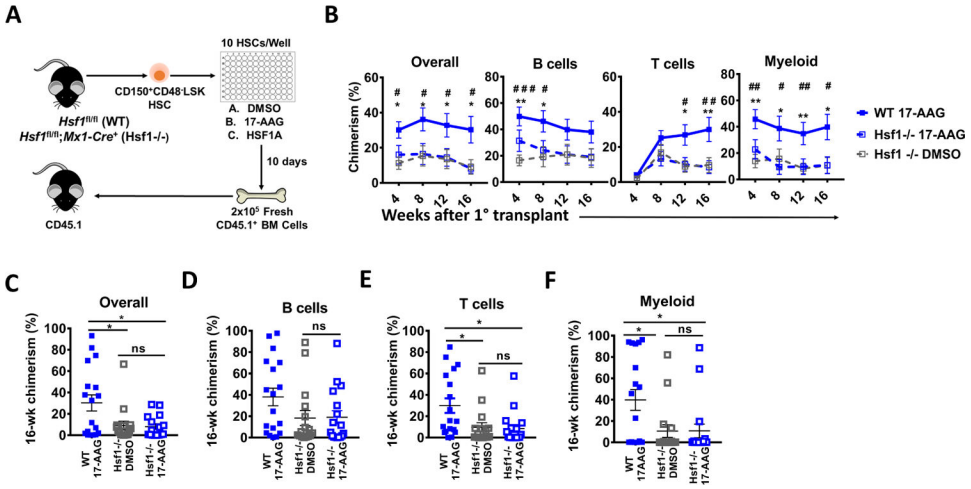

Figure 5. 17-AAG promotes ex vivo HSC maintenance in an Hsf1 dependent manner.

(A) Strategy to test if 17-AAG and HSF1A promote maintenance of cultured HSCs in an Hsf1 dependent manner. (B) Donor cell engraftment when 10 *Hsf1*$^{fl/fl}$ (WT) or *Hsf1*$^{fl/fl}$;Mx1-*Cre*$^{+}$ (*Hsf1*$^{-/-}$) HSCs were cultured for 10d in basic HSC medium supplemented with DMSO or 17-AAG and transplanted with 2×10^{5} recipient-type bone marrow cells into irradiated mice. Total hematopoietic, B-, T- and myeloid cell engraftment are shown (n=4 donors, 16–18 recipients/condition). (C-F) Long-term donor (C) hematopoietic, (D) B-, (E) T- and (F) myeloid cell engraftment in the peripheral blood of individual recipient mice from transplants in panel B. Data represent mean ± SEM (B-F). Significance was assessed using a t-test (*P<0.05; **P<0.01, ***P<0.001).

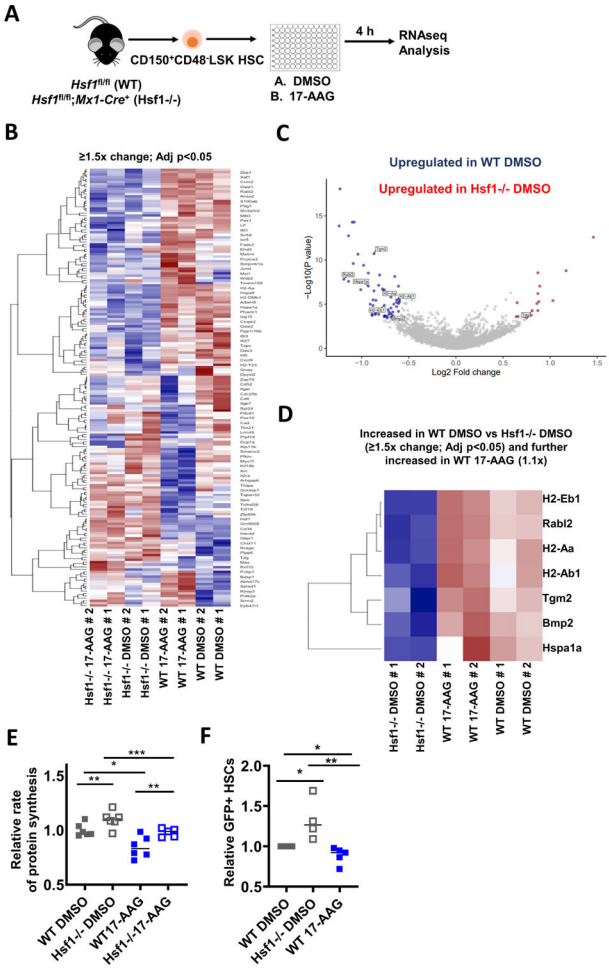

Figure 6. Hsf1 and 17-AAG induce transcriptional changes and promote proteostasis maintenance in ex vivo cultured HSCs.

(A) Strategy to compare gene expression profiles in *Hsf1*$^{fl/fl}$ (WT) and *Hsf1*$^{fl/fl}$;Mx1-*Cre*$^{+}$ (*Hsf1*$^{-/-}$) HSCs cultured for 4h in the presence or absence of 17-AAG. (B) Heat map showing differentially expressed transcripts (≥1.5-fold change; Padj<0.05) between WT and *Hsf1*$^{-/-}$ HSCs cultured for 4h with 17-AAG or DMSO (n=2). (C) Volcano plot showing differentially expressed transcripts in cultured (4h) WT and *Hsf1*$^{-/-}$ HSCs. Genes significantly upregulated in WT HSCs are shown in blue and in *Hsf1*$^{-/-}$ HSCs are shown in red. (D) Heat map showing the subset of genes whose expression is significantly upregulated (≥1.5-fold change; Padj<0.05) in WT as compared to *Hsf1*$^{-/-}$ cultured HSCs and that exhibit further increased expression (≥1.1-fold) in WT HSCs cultured with 17-AAG. (E) Protein synthesis in WT and *Hsf1*$^{-/-}$ CD48^{-}LSK cells cultured for 4h in basic HSC medium supplemented with DMSO or 17-AAG (n=5–6/genotype/condition). (F) Relative frequency of GFP^{+} HSCs after culture (18h) of Ub^{G76V}-*GFP* (DMSO and 17-AAG) and *Hsf1*$^{-/-}$;Ub^{G76V}-*GFP* HSCs (n=4–5/condition). Data represent mean ± SD (E,F). Significance was assessed using a t-test (E,F; *P<0.05; **P<0.01, ***P<0.001).

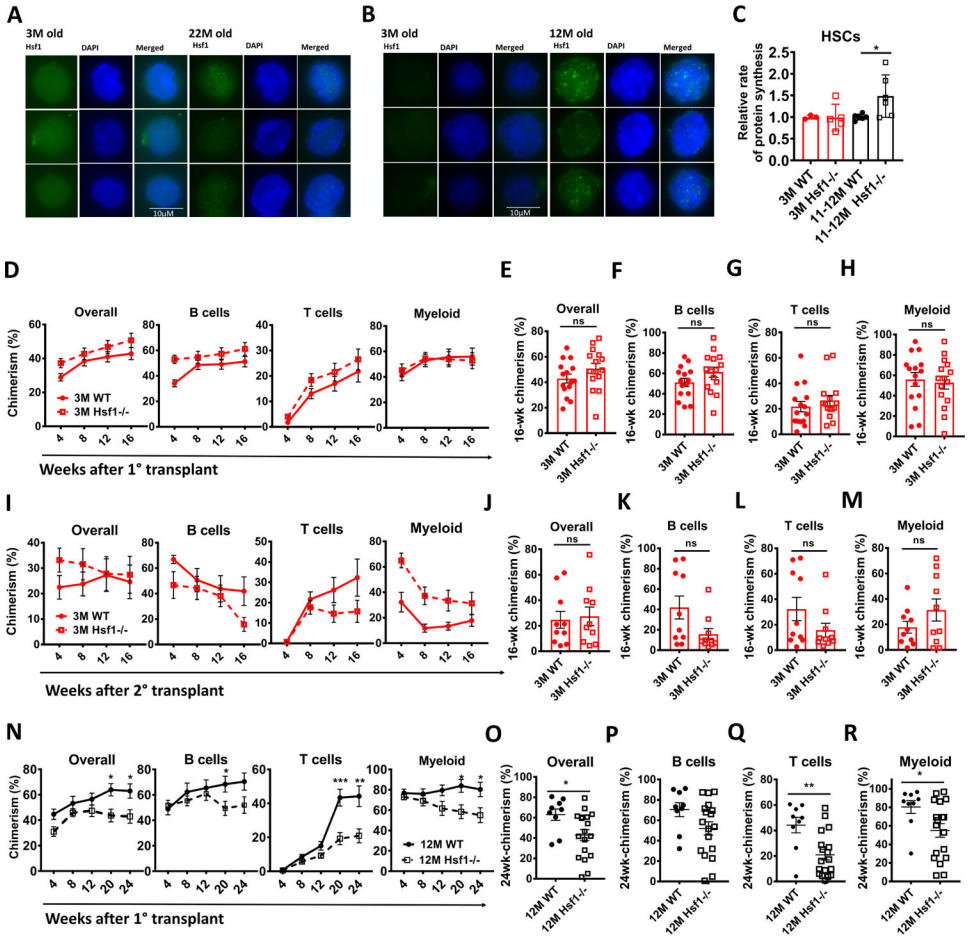

Figure 7. *Hsf1* deficiency impairs HSC function during aging.

(A,B) Representative immunofluorescence staining examining Hsf1 expression in fresh CD48-LSK cells from 3-month-, (A) 22-month- and (B) 12-month-old mice. (C) Relative protein synthesis in HSCs in 3-month- and 11–12-month-old *Hsf1*$^{fl/fl}$ (WT) or *Hsf1*$^{fl/fl}$;Mx1-*Cre*$^{+}$ (*Hsf1*$^{-/-}$) mice in vivo (n=3–8 mice/genotype/age). (D) Donor cell engraftment when 5×10^5 2-month-old old WT or *Hsf1*$^{-/-}$ bone marrow cells were transplanted with 5×10^5 recipient-type bone marrow cells into irradiated mice. Total hematopoietic, B-, T- and myeloid cell engraftment are shown (n=3 donors, 15 recipients/condition). (E-H) Long-term donor (E) hematopoietic, (F) B-, (G) T- and (H) myeloid cell engraftment in the peripheral blood of individual mice from transplants in D. (I) Donor cell engraftment after serial transplantation of 3×10^6 bone marrow cells from primary recipients in D into secondary recipients. Total hematopoietic, B-, T- and myeloid cell engraftment are shown (n=2 donors,10 recipients/condition). (J-M) Long-term donor (J) hematopoietic, (K) B-, (L) T- and (M) myeloid cell engraftment in the peripheral blood of individual recipient mice from transplants in I. (N) Donor cell engraftment when 5×10^5 10–12-month-old WT or *Hsf1*$^{-/-}$ bone marrow cells were transplanted with 5×10^5 recipient-type bone marrow cells into irradiated mice. Total hematopoietic, B-, T- and myeloid cell engraftment are shown (n=2–4 donors, 10–18 recipients/condition). (O-R) Long-term (24-week) donor (O) hematopoietic, (P) B-, (Q) T- and (R) myeloid cell engraftment in the blood of individual mice from

transplants in N. Data represent mean ± SD (C) or ± SEM (D–R). Significance was assessed using a t-test (*P<0.05; **P<0.01, ***P<0.001).

KEY RESOURCES TABLE

REAGENT or RESOURCE	SOURCE	IDENTIFIER
Antibodies		
APC Anti-mouse CD3ε (17A2)	BioLegend	Cat #100236; RRID:AB_2561456
FITC Anti-mouse CD3ε (17A2)	BioLegend	Cat #100204; RRID:AB_312661
PE Anti-mouse CD3ε (17A2)	BioLegend	Cat #100206; RRID:AB_312663
APC Anti-mouse CD4 (GK1.5)	BioLegend	Cat #100412; RRID:AB_312697
FITC Anti-mouse CD4 (GK1.5)	BioLegend	Cat #100406; RRID:AB_312691
PE Anti-mouse CD4 (GK1.5)	BioLegend	Cat #100408; RRID:AB_312693
APC Anti-mouse CD5 (53-7.3)	BioLegend	Cat #100626; RRID:AB_2563929
FITC Anti-mouse CD5 (53-7.3)	BioLegend	Cat #100606; RRID:AB_312735
PE Anti-mouse CD5 (53-7.3)	BioLegend	Cat #100608; RRID:AB_312737
APC Anti-mouse CD8α (53-6.7)	eBioscience	Cat #17-0081-82; RRID:AB_469335
FITC Anti-mouse CD8α (53-6.7)	eBioscience	Cat #11-0081-85; RRID:AB_464916
PE Anti-mouse CD8α (53-6.7)	eBioscience	Cat #12-0081-83; RRID:AB_465531
APC Anti-mouse CD11b (M1/70)	eBioscience	Cat #17-0112-82; RRID:AB_469343
APC efluor780 Anti-mouse CD11b (M1/70)	eBioscience	Cat #47-0112-82; RRID:AB_1603093
FITC Anti-mouse CD11b (M1/70)	eBioscience	Cat #12-0112-83; RRID:AB_2734870
PE Anti-mouse CD11b (M1/70)	eBioscience	Cat #11-0112-85; RRID:AB_464936
PE/Cy7 Anti-mouse CD16/32 (FcγRII/III; 93)	BioLegend	Cat #101318; RRID:AB_2104156
PerCP/Cy5.5 Anti-mouse CD16/32 (FcγRII/III; 93)	BioLegend	Cat #101324; RRID:AB_1877267
Biotin Anti-mouse CD34 (RAM34)	eBioscience	Cat #13-0341-85; RRID:AB_466426
eFluor660 Anti-mouse CD34 (RAM34)	eBioscience	Cat #50-0341-82; RRID:AB_10596826
Alexa Fluor 700 Anti-mouse CD34 (RAM34)	eBioscience	Cat #56-0341-82; RRID:AB_493998
FITC Anti-mouse CD34 (RAM34)	eBioscience	Cat #11-0341-85; RRID:AB_465022
APC Anti-mouse CD41 (MWReg30)	Biolegend	Cat #133913; RRID:AB_11126751
FITC Anti-mouse CD43 (R2/60)	eBioscience	Cat #11-0431-85; RRID:AB_465041
PE Anti-mouse CD43 (R2/60)	eBioscience	Cat #12-0431-83; RRID:AB_465660
APC eFluor 780 Anti-mouse CD45.1 (A20)	eBioscience	Cat #47-0453-82; RRID:AB_1582228
Alexa Fluor 700 Anti-mouse CD45.2 (104)	BioLegend	Cat #109822; RRID:AB_493731
FITC Anti-mouse CD45.2 (104)	BioLegend	Cat #109806; RRID:AB_313443
APC Anti-mouse CD45R (B220) (RA3-6B2)	eBioscience	Cat #17-0452-83; RRID:AB_469396
FITC Anti-mouse CD45R (B220) (RA3-6B2)	eBioscience	Cat #11-0452-85; RRID:AB_465055
PE Anti-mouse CD45R (B220) (RA3-6B2)	eBioscience	Cat #12-0452-85; RRID:AB_465673
PerCP-Cyanine5 Anti-mouse CD45R (B220) (RA3-6B2)	eBioscience	Cat #45-0452-82; RRID:AB_1107006
APC Anti-mouse CD48 (HM48-1)	BioLegend	Cat #103412; RRID:AB_571997
FITC Anti-mouse CD48 (HM48-1)	BioLegend	Cat #103404; RRID:AB_313019
PE Anti-mouse CD48 (HM48-1)	BioLegend	Cat #103406; RRID:AB_313021
PE/Cy7 Anti-mouse CD48 (HM48-1)	BioLegend	Cat #103424; RRID:AB_2075049

REAGENT or RESOURCE	SOURCE	IDENTIFIER
FITC Anti-mouse CD71 (R17217)	eBioscience	Cat #11-0711-85; RRID:AB_465125
APC Anti-mouse CD117 (cKit) (2B8)	eBioscience	Cat #17-1171-83; RRID:AB_469431
APC eFluor 780 Anti-mouse CD117 (cKit) (2B8)	eBioscience	Cat #47-1171-82; RRID:AB_1272177
PE-Cyanine7 Anti-mouse CD117 (cKit) (2B8)	eBioscience	Cat #25-1171-82; RRID:AB_469644
PE Anti-mouse CD127 (IL7Rα; A7R34)	BioLegend	Cat #135010; RRID:AB_1937251
APC Anti-mouse CD150 (TC15-12F12.2)	BioLegend	Cat #115910; RRID:AB_493460
PE Anti-mouse CD150 (TC15-12F12.2)	BioLegend	Cat #115904; RRID:AB_313683
PE-Cyanine7 Anti-mouse CD150 (TC15-12F12.2)	BioLegend	Cat #115914; RRID:AB_439797
APC Anti-mouse Ter119 (TER-119)	Biolegend	Cat #116212; RRID:AB_313713
FITC Anti-mouse Ter119 (TER-119)	Biolegend	Cat #116206; RRID:AB_313709
PE Ter119 (TER-119)	Biolegend	Cat #116208; RRID:AB_313709
APC Anti-mouse Sca-1 (D7, E13-161.7)\	eBioscience	Cat #17-5981-82; RRID:AB_469487
Alexa Fluor 700 Anti-mouse Sca-1 (D7, E13-161.7)	eBioscience	Cat #56-5981-82; RRID:AB_657836
FITC Anti-mouse Sca-1 (D7, E13-161.7)	eBioscience	Cat #11-5981-85; RRID:AB_465334
PerCp-Cyanine5.5 Anti-mouse Sca-1 (D7, E13-161.7)	eBioscience	Cat #45-5981-82; RRID:AB_914372
APC Anti-mouse Gr-1 (RB6-8C5)	BioLegend	Cat #108412; RRID:AB_313377
FITC Anti-mouse Gr-1 (RB6-8C5)	BioLegend	Cat #108406; RRID:AB_313371
PE Anti-mouse Gr-1 (RB6-8C5)	BioLegend	Cat #108408; RRID:AB_313373
PE/Cy7 Anti-mouse Gr-1 (RB6-8C5)	BioLegend	Cat #108416; RRID:AB_312663
APC Anti-mouse IgM (II/41)	eBioscience	Cat #17-5790-82; RRID:AB_469458
PE Anti-mouse IgM (II/41)	eBioscience	Cat #12-5790-83; RRID:AB_465941
Streptavidin-PECy7	BioLegend	Cat #405206; RRID:AB_2892630
APC Anti-human CD34 (581)	BD	Cat #555824; RRID:AB_398614
anti-Hsf1 Rabbit polyclonal	Cell Signaling	Cat #4356S; RRID:AB_2120258
Alexa 488 conjugated anti-Rabbit A21206,	Invitrogen	Cat #A-21206; RRID:AB_2535792
Chemicals, Peptides, and Recombinant Proteins		
PIPC	GE Healthcare Biosciences Corp	Cat #27473201
Anti-mouse CD117 microbeads	Miltenyi	Cat #130-091-224
OP-Puro	Medchem Source	Custom Synthesized
2-mercaptoethanol	Sigma	Cat #M3148
StemSpan	StemCell Technologies	Cat #09650
Human SCF	PeproTech	Cat #300-07
Human Fms-related tyrosine kinase 3 ligand Flt3-l	PeproTech	Cat #300-19
Human TPO	PeproTech	Cat #300-18
Trypan Blue	Corning	Cat #25-900-CI
F-12 medium	Life Technologies	Cat #21041025
Insulin-Transferrin-Selenium-Ethanolamine (ITS-X)	Life Technologies	Cat #51500056
HEPES	Life Technologies	Cat #15630106
Penicillin/streptomycin/glutamine	Life Technologies	Cat #10378016

REAGENT or RESOURCE	SOURCE	IDENTIFIER
Polyvinyl Alcohol (PVA)	Sigma	Cat #501784760
Hank's buffered salt solution (HBSS)	Corning	Cat #MT21022CV
Heat-inactivated bovine serum	Gibco	Cat #26170043
Prime-XV	Prototype; Irvine Scientific	Cat #91206
Mouse SCF	PeproTech	Cat #250-03
Mouse TPO	PeproTech	Cat #315-14
17-AAG	SelleckChem	Cat #S1141
HSF1A	Axon MedChem	Cat #1890
DMSO	Sigma	Cat #D2650
Baytril	Covetrus	Cat #37713
Ammonium chloride potassium buffer		
Methylcellulose culture medium M3434	STEMCELL Technologies	Cat #03434
Paraformaldehyde	Affymetrix	Cat #19943
PBS	Corning	Cat #MT21040CV
Tween 20	Sigma	Cat #P9416
4',6-diamidino-2-phenylindole (DAPI)	Life Technologies	Cat #62247
Vectashield	Vector Laboratories	Cat #H-1000
Saponin	Sigma	Cat #47036
Fetal Bovine Serum	Life Technologies	Cat #16000044
G-CSF Zarxio, PFS	McKesson Medical-Surgical Inc.	Cat #1113496
Cyclophosphamide	McKesson Medical-Surgical Inc.	Cat #952047
Critical Commercial Assays		
Click-iT Cell Reaction Buffer Kit	Life Technologies	Cat #C10269
Alexa Fluor 555-conjugated azide	Life Technologies	Cat #A20012
Proteasome-Glo chymotrypsin-like cell based assay	Promega	Cat #G8660
RNeasy Plus Micro Kit	Qiagen	Cat #74034
Deposited Data		
RNA-sequencing data	GEO	GSE179415
Experimental Models: Cell Lines/Primary Cells		
Cord blood derived CD34+ cells	All Cells	N/A
Experimental Models: Organisms/Strains		
Mouse: B6: C57BL/6J	The Jackson Laboratory	Cat #000664; RRID:IMSR_JAX:000664
Mouse: B6SJL: B6.SJL	The Jackson Laboratory	Cat #002014; RRID:IMSR_JAX:002014
Mouse: Ub^{G76V}-*GFP*	The Jackson Laboratory	Cat #008111; RRID:IMSR_JAX:008111
Mouse*: Hsf1*^{fl}	Le Masson et al, 2011	N/A
Software and Algorithms		
FlowJo	FlowJo, LLC	N/A
FACSDiva	BD Bioscience	N/A

REAGENT or RESOURCE	SOURCE	IDENTIFIER
Prism 8	GraphPad	N/A
ImageJ	NIH	N/A
Image Lab 6.0.1	Bio-Rad	N/A
TopHat 1.4.1	JHU CCB	N/A
STAR 2.6.1	N/A	N/A
PRINSEQ Lite 0.20.3	N/A	N/A
Htseq-count 0.7.1	N/A	N/A
featureCounts 1.6.5	N/A	N/A
Bioconductor package DESeq2 1.24.0	Bioconductor	N/A
Matplotlib	J.D Hunter, 2007	N/A
ELDASoftware	Hu and Smyth, 2009	N/A
Keyence Microscope Software	Keyence	N/A